New Horizons in Science and Mathematics 2019

Editors

Prof. Dr. Hüsniye AKA SAĞLIKER
Dr. Öğr. Gör. Abdurrahman Günday

Gece Akademi

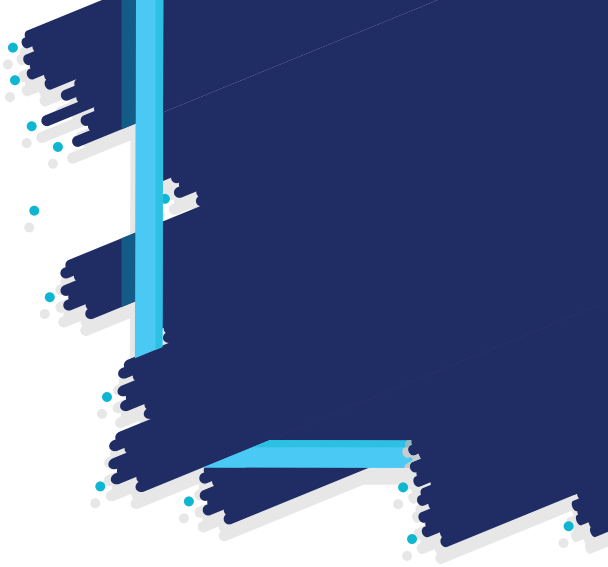

New Horizons in Science and Mathematics

GECE AKADEMİ

İmtiyaz Sahibi / Publisher • Gece Kitaplığı
Genel Yayın Yönetmeni / Editor in Chief • Doç. Dr. Atilla ATİK
Editörler / Editors •
Prof. Dr. Hüsniye AKA SAĞLIKER
Dr. Öğr. Gör. Abdurrahman Günday
Kapak & İç Tasarım / Cover & Interior Design • Didem S. KORKUT
Sosyal Medya / Social Media • Arzu Betül ÇUHACIOĞLU

Birinci Basım / First Edition • ©EKİM 2019

ISBN • 978-605-80229-4-2

Gece Kitaplığı / Gece Publishing
ABD Adres/ USA Address: 387 Park Avenue South, 5th Floor,
New York, 10016, USA
Telefon / Phone: +1 347 355 10 70
Türkiye Adres / Turkey Address: Kızılay Mah. Fevzi Çakmak 1. Sokak
Ümit Apt. No: 22/A Çankaya / Ankara / TR
Telefon / Phone: +90 312 384 80 40
+90 555 888 24 26
web: www.gecekitapligi.com
e-mail: geceakademi@gmail.com

GECE AKADEMİ

Baskı & Cilt / Printing & Volume
Sertifika / Certificate No:29377

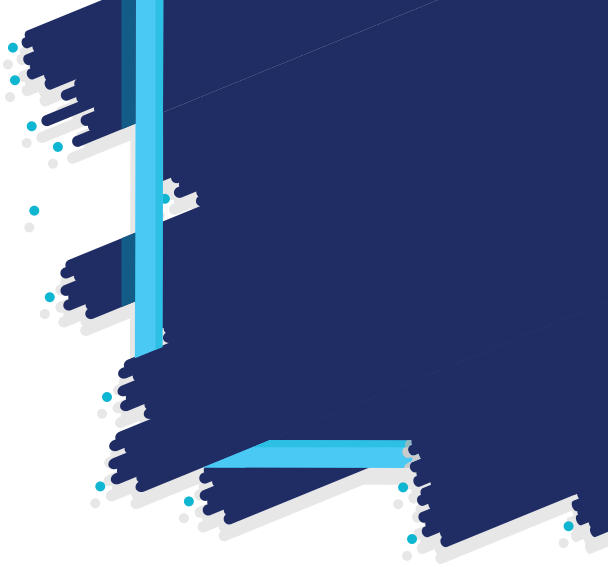

New Horizons in Science and Mathematics

GECE AKADEMİ

CONTENTS

DFT CALCULATIONS OF 3-METHOXY-2-[(E)-(4-METHOXYPHENYL)-IMINOMETHYL]PHENOL

Gonca ÖZDEMİR TARI[1]

1 Vezirköprü Vocational School, Ondokuz Mayıs University, 55900, Samsun, Turkey

DFT CALCULATIONS OF 3-METHOXY-2-[(E)-(4-METHOXYPHENYL)-IMINOMETHYL]PHENOL

Gonca ÖZDEMİR TARI[1]

1. INTRODUCTION

The Schiff base compounds have a broad range of application in the fields of coordination and medical chemistry, synthesis of new drugs, dyes and optical materials industries [1-6]. Schiff base compounds exhibit tautomeric form because of transferring a proton intramolecular between the phenol-imine (O-H...N) [7-8], keto-amine (N-H..O) [9-10] and zwitterionic forms (N^+-H..O^-) [11-13]. Density functional theory (DFT) is becoming more useful to experimentalists in computing the geometrical parameters and other properties like vibrational, thermal, non-linear, optical etc. of polyatomic molecules [14]. In a previously published study, 3-methoxy-2-[(E)-(4-methoxyphenyl)-iminomethyl] phenol ($C_{15}H_{15}NO_3$) was synthesized and characterized by X-ray diffraction technique [15]. The purpose of this manuscript was to investigate the physicochemical properties of the corresponding compound, using DFT method. Therefore, it was conducted in this study to determine the molecular structure and geometry, frontier molecular orbitals (FMOs), molecular electrostatic potential (MEP), natural bond orbitals (NBO), non-linear optical properties (NLO) and thermodynamic properties using B3LYP and B3PW91 methods. The comparison between the theoretical calculations and experimental results revealed that parameters showed that DFT/B3LYP/6-311++G(d,p) predictions were in good agreement with the experimental data. These studies are valuable for understanding the molecular properties of the Schiff base compounds and for synthesizing new compounds in the future.

1 Vezirköprü Vocational School, Ondokuz Mayıs University, 55900, Samsun, Turkey

2. Computational methods

Quantum chemical calculations were carried using the DFT method with the B3LYP [16-17] and B3PW91 [18-20] with the 6-311++G(d,p) levels by using Gaussian 03W software [21] and the GaussView molecular visualization program [22]. The molecular energy profile of the molecule was obtained as a function of the selected torsion angle by a rotation around the bond in range from -180^0 to 180^0 and step size of 10^0. In addition, the HOMO and LUMO energies, dipole moment (μ), chemical hardness(η) and softness (S), etc. of energetic behaviors of the molecule in various solvent media were obtained using the integral equation formalism polarizable continuum model (IEF-PCM) [23] and the Onsager method [24]. Furthermore, the net charges was calculated with Mulliken Population Method and Natural Population Analysis was performed. The obtained natural atomic charge values from the NPA procedures were obtained from NBO analysis. Recent studies were emphasized the importance of calculating the electronic and structural properties of the organic compounds with different theoretical methods [25-28].

3. Result and Discussion

3.1. Molecular structure

The optimized parameters of the molecule were carried using theoretical methods. The title compound adopts the enol-imine tautomeric form. The bond lengths of C7=N1 (1.278(3) Å) and C8=N1 (1.419(2) Å) have double-bond characteristics while the bond length between C6-O2 (1.356 (2) Å) is a typical single bond [15]. These experimental values are similar to that calculated results; 1.288 Å, 1.407 Å and 1.345 Å in optimized geometry for the B3LYP method; 1.288 Å, 1.401 Å and 1.337 Å for the B3PW91 method, respectively. The optimized bond

lengths of C-C in the phenyl rings fall in the range 1.381-1.449 Å for the B3LYP method; 1.379-1.445 Å for the B3PW91 method, respectively. The experimental [15] and calculated geometric parameters were also compared and given in Table 1. According to Table 1, the experimentally obtained geometrical parameters were incoherent with the calculated results.

Table 1. *Selected molecular structure parameter for the title compound.*

Parameters	Experimental	B3LYP 6-311G++(d,p)	B3PW91 6-311G++(d,p)
Bond Lengths (Å)			
C1-C2	1.407(3)	1.414332	1.41129
C2-C3	1.373(3)	1.38493	1.38287
C3-C4	1.393(3)	1.40578	1.40407
C4-C5	1.369(3)	1.38177	1.37943
C5-C6	1.381(3)	1.40220	1.40081
C6-C1	1.407(3)	1.41361	1.41206
C1-C7	1.451(3)	1.44981	1.44507
C3-O1	1.375(3)	1.37034	1.36398
C7-N1	1.278(3)	1.28883	1.28802
C8-N1	1.419(2)	1.40730	1.40180
C6-O2	1.356(2)	1.34527	1.33753
C8-C9	1.391(3)	1.40506	1.40271
C9-C10	1.366(3)	1.38348	1.38120
C10-C11	1.393(3)	1.40155	1.39956
C11-C12	1.386(3)	1.39709	1.39514
C12-C13	1.384(3)	1.39531	1.39267
C13-C8	1.385(3)	1.39850	1.39629
C11-O3	1.369(2)	1.36427	1.35797
C14-O3	1.419(3)	1.42095	1.41346
C15-O1	1.397(3)	1.41832	1.41084
Max. Diff.		***0.02132***	***0.01981***
RMSE		***0.0120***	***0.0112***
Bond Angles (°)			
C6-C1-C2	118.79(19)	119.51502	119.73993
C6-C1-C7	121.21(19)	121.32513	120.91231
C2-C1-C7	119.91(19)	119.15950	119.34738
C3-C2-C1	120.7(2)	120.72724	120.65993
C2-C3-O1	125.3(2)	125.18373	125.16165
C2-C3-C4	119.3(2)	119.19267	119.11347
O1-C3-C4	115.40(19)	115.62359	115.72488

C5-C4-C3	121.0(2)	120.87141	120.99130
C4-C5-C6	120.4(2)	120.68451	120.68144
O2-C6-C5	118.21(18)	118.62799	118.98761
O2-C6-C1	122.03(19)	122.36308	122.19878
C5-C6-C1	119.75(19)	119.00887	118.81353
N1-C7-C1	120.8(2)	122.51220	122.15910
C13-C8-C9	118.6(2)	118.32064	118.33387
C13-C8-N1	123.71(18)	123.61706	123.49867
C9-C8-N1	117.54(19)	118.02150	118.12867
C10-C9-C8	120.9(2)	120.95271	120.93560
C9-C10-C11	120.29(19)	120.28526	120.30311
Max. Diff.		***1.7122***	***1.3591***
RMSE		***0.566***	***0.542***
Torsion Angles (°)			
C1-C2-C3-C4	1.0(3)	-0.00990	-0.03021
C6-C1-C2-C3	-1.5(3)	-0.13256	-0.14379
C7-C1-C2-C3	175.00(19)	-179.92105	-179.92243
C1-C2-C3-O1	-177.7(2)	179.99677	179.97350
C2-C3-C4-C5	-0.1(3)	0.08641	0.11294
O1-C3-C4-C5	178.7(2)	-179.91963	-179.89043
C3-C4-C5-C6	-0.2(3)	-0.01806	-0.01889
C4-C5-C6-O2	-179.4(2)	179.79237	179.74334
C6-C1-C7-N1	-6.4(3)	-0.73540	-0.79134
C2-C1-C7-N1	177.11(18)	179.04913	178.98463
N1-C8-C9-C10	176.32(19)	-179.88559	-179.78853
C10-C11-O3-C14	179.2(2)	-179.77069	-179.79516
C2-C3-O1-C15	-2.2(4)	-0.31900	-0.27646
C1-C7-N1-C8	172.99(18)	177.24600	177.15863
C7-N1-C8-C9	148.9(2)	147.02862	146.73536

Aromaticity/aromatic belongs to one of the most useful and popular terms in organic chemistry and related fields [29]. The HOMA (harmonic oscillator model of aromaticity) value is an indicator that defines the aromaticity by using bond-length [30-31]. Homa index was calculated using the following equation 1 for rings [30],

$$HOMA = 1 - \left[\frac{\alpha}{n} \sum_{i=1}^{n} (R_i - R_{opt})^2 \right] \quad (1)$$

n is the number of bonds in the molecular structure, α is the normalization constant and the optimal value R_{opt}

(α=257.7 and R_{opt}=1.388 Å for C-C bonds) [31]. If the calculated HOMA index is in the range of 0.900-0.990 then the ring is aromatic, but if the calculated HOMA index is in the range of 0.500-0.800 then the ring is non-aromatic [32-33]. The calculated HOMA index of C1-C6 and C8-C11 phenyl rings are 0.940 and 0.976; respectively. These results demonstrated a high aromatic character for both rings. The compound adopts E configuration about the C=N double bond and has two phenyl rings, C1-C6 and C8-C13 (Figure 1). This intramolecular O—H···N hydrogen bond results in the formation of an S(6) ring [34-35]. The two phenyl rings are twisted with respect to each other making dihedral angle of 44.08(5)^0 for the X-ray [15], 36.66^0 for the B3LYP method and 37.03^0 for the B3PW91 method, respectively. The non-planarity molecules show the photochromic properties. The dihedral angle of the molecule supported the photochromic tendency.

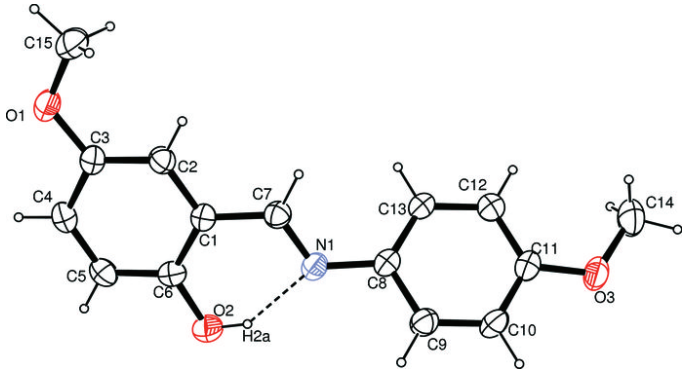

Figure 1. *The molecular structure of the title compound, $C_{17}H_{19}O_3N_3$, showing the atom-numbering scheme and 30% probability displacement ellipsoids.*

The bond lengths and angles are slightly different from the experimental data. Because the existence of the crystal field in the solid state form have connected with the molecules together along with the intermolecular interactions. These interactions reveal different geometric parameters

between the calculated and experimental values [36]. The superimposed molecular skeleton obtained from X-ray diffraction is a logical method for the comparison of the structure obtained from the theoretical calculation (Figure 2). The computed root mean square error (RMSE) values were 0.231 and 0.236 for the B3LYP and B3PW91 methods, respectively. According to the results, the B3LYP method is better than the B3PW91 method in predicting the geometric parameters of the molecule.

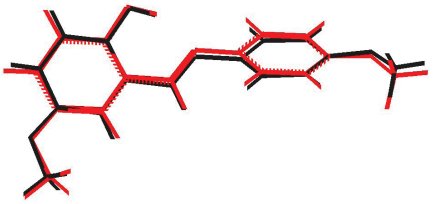

B3LYP

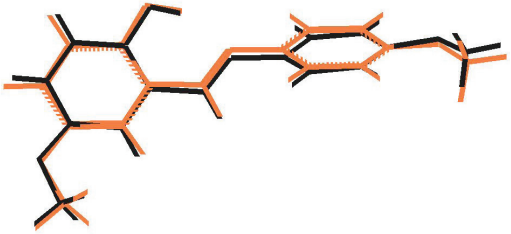

B3PW91

Figure 2. *Atom-by-atom superimposition of the calculated structure (red) over the X-ray structure (black) for the title compound.*

In order to determine the minimum energy conformer, selected torsion angle are varied from -180 to +180 in every 10^0. It was chosed because the torsion angle T(C7-N1-C8-C9) connected the two aromatic rings (Figure 3). This angle was $148.9(2)^0$ for X-ray and 147.02^0 for B3LYP method. The Figure 3 shows two minima at $\pm 90^0$ and one

maxima at 30^0. These energy values were 0.0702738 and 0.0725821 Hartree, respectively. These minumum conformations become the most stable state of the molecule.

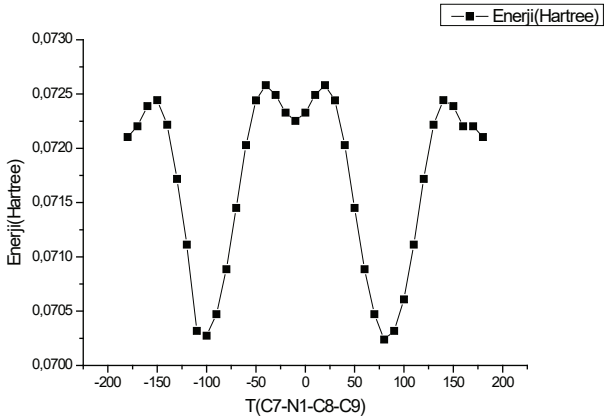

Figure 3. *The molecular energy profile of the optimized counterpart of the title compound versus selected degrees of torsional freedom.*

3.2. Frontier molecular orbitals analysis

The HOMO represents the capability to donate an electron; LUMO represents the capability to receive an electron. A molecule with small frontier orbital gap is generally associated with a high chemical reactivity, low kinetic stability and is also termed as soft molecule [37]. A hard molecule has a large HOMO-LUMO gap. Chemical hardness is one of the highly useful concepts which enable chemists to understand reactivities without reference to large supercomputers and databases [38]. Soft systems are large and highly polarizable, while hard systems are relatively small and much less polarizable [39]. The electrophilicity index, is a measure of energy lowering due to maximal electron flow between donor and acceptor [40]. FMOs energies of the molecule, which has 136 electrons, 68 occupied molecular orbitals, were performed using the same methods. The

computed HOMO and LUMO energies show the chemical activity of the molecule. The energy levels of the HOMO-1, HOMO, LUMO and LUMO+1 orbitals for the molecular structure are shown in Figure 4. As can be clearly seen from the figure, in the HOMO, HOMO-1 and LUMO electrons are extended over the entire molecule, and in the LUMO+1 are mainly delocalized on the C8-C13 phenyl ring.

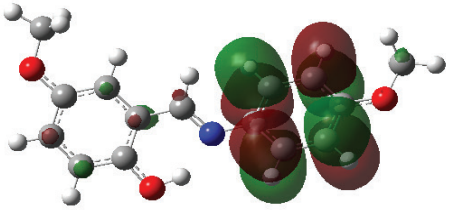

LUMO+1

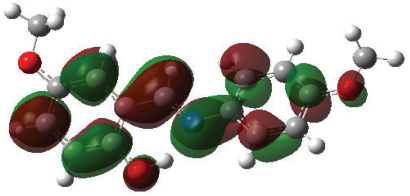

LUMO

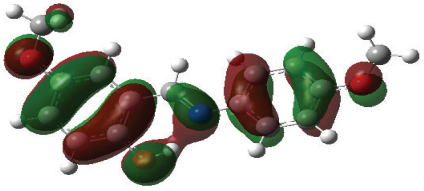

HOMO

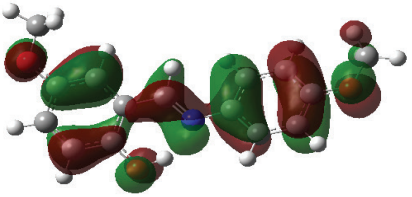

HOMO-1

Figure 4. *Molecular orbital surfaces and energy levels given in parentheses for the HOMO, HOMO-1 LUMO and LUMO+1 of the title compound computed at B3LYP/6-311G++(d,p) level.*

In addition; the other electronic structure parameters were calculated in solvent media, and the results given in Table 2. As can be seen in Table 2, the obtained E_{TOTAL} and S of the title compound also decreasewith the increasing polarity of the solvent. The μ values obtained by the Onsager method are slightly different from the IEF-PCM method. The μ values obtained from the two approaches increase with the increasing of the solvent polarity.

3.3. The solvent effect on the nonlinear optical properties

Schiff base compounds have been recently investigated for potential applicability in optical communication and have many NLO behaviors [41-50]. Nonlinear optics deals with the interaction of applied electromagnetic fields in various materials

to generate new electromagnetic fields, altered in frequency, phase, or other physical properties [51]. Organic molecules able to manipulate photonic signals efficiently are of importance in technologies such as optical communication, optical computing and dynamic image processing [52]. On the other hand, the linear polarizability is less affected by the solvent than the higher order polarizabilities [53]. In order to investigate the NLO properties of the title compound, the components of the dipole moment (μ), linear polarizability (α), anisotropy of the polarizability (Δα) and first hyperpolarizability (β) were calculated in the solvent media with the same methods, and were given in Table 3.

Table 2. *The calculated total molecular energies (Hartree), dipole moments (Debye), frontier orbital energies (eV), ionization energy (eV), electron affinity (eV), electronegativity (eV), hardness (eV) and softness (eV^{-1}) for the title compound using B3LYP and B3PW91 methods with the 6-311++G(d,p).*

	ε	E_{TOTAL}	μ	ΔE	I	A	χ	η	S	ω
B3LYP	ε = 1	-861.2639	4.8782	3.6755	5.6282	1.9527	3.7904	1.8377	0.2720	-3.9089
	ε = 4.9	-861.2752	5.9868	3.7256	5.7175	1.9919	3.8547	1.8628	0.2684	-3.9882
IEF-PCM	ε = 10.36	-861.2780	6.2991	3.7384	5.7417	2.0033	3.8725	1.8692	0.2674	-4.0114
	ε = 24.55	-861.2799	6.5173	3.7477	5.7534	2.0057	3.8737	1.8742	0.2667	-4.0031
	ε = 46.7	-861.2804	6.5780	3.7495	5.7618	2.0123	3.8870	1.8747	0.2667	-4.0296
	ε = 78.39	-861.2813	6.6468	3.7539	5.7602	2.0063	3.8832	1.8769	0.2663	-4.0170
	ε = 4.9	-861.2657	5.9856	3.6760	5.6671	1.9911	3.8291	1.8380	0.2720	-3.9885
	ε = 10.36	-861.2661	6.2761	3.6714	5.6742	2.0028	3.8385	1.8357	0.2723	-4.0132
ONSAGER	ε = 24.55	-861.2664	6.4551	3.6674	5.6775	2.0101	3.8438	1.8337	0.2726	-4.0286
	ε = 46.7	-861.2665	6.5226	3.6658	5.6786	2.0128	3.8457	1.8329	0.2727	-4.0344
	ε = 78.39	-861.2665	6.5539	3.6646	5.6788	2.0142	3.8465	1.8323	0.2728	-4.0374
B3PW91	ε = 1	-860.9192	4.8607	3.6706	5.6707	1.9701	3.8054	1.8353	0.2724	-3.9451
	ε = 4.9	-860.9308	5.9721	3.7199	5.7458	2.0259	3.8858	1.8599	0.2688	-4.0592
	ε = 10.36	-860.9337	6.2820	3.7329	5.7735	2.0406	3.9070	1.8664	0.2678	-4.0893
IEF-PCM	ε = 24.55	-860.9356	6.4952	3.7419	5.7882	2.0463	3.9172	1.8709	0.2672	-4.1008
	ε = 46.7	-860.9362	6.5579	3.7441	5.7964	2.0523	3.9243	1.8720	0.2670	-4.1132
	ε = 78.39	-860.9370	6.6263	3.7482	5.7967	2.0485	3.9226	1.8741	0.2667	-4.1051
	ε = 4.9	-860.9112	6.0591	3.6723	5.6859	2.0136	3.8497	1.8361	0.2723	-4.0357
	ε = 10.36	-860.9217	6.3829	3.6671	5.6943	2.0272	3.8607	1.8335	0.2727	-4.0646
ONSAGER	ε = 24.55	-860.9220	6.5847	3.6614	5.6979	2.0365	3.8672	1.8307	0.2731	-4.0845
	ε = 46.7	-860.9221	6.6613	3.6598	5.6990	2.0392	3.8691	1.8299	0.2732	-4.0903
	ε = 78.39	-860.9221	6.6969	3.6583	5.6992	2.0409	3.8700	1.8291	0.2733	-4.0940

$$\Delta E = \left|E_{HOMO} - E_{LUMO}\right|,\ I = -E_{HOMO},\ A = -E_{LUMO},\ \chi = \frac{I + A}{2},\ \eta = \frac{I - A}{2},\ S = \frac{1}{2\eta},\ \omega = -\frac{\chi^2}{2\eta}$$

Table 3. *The calculated values of μ (D), α (Å³), Δα (Å³) and β (x10⁻³⁰esu) for the title compound in different solvents.*

		Gas phase ($\varepsilon = 1$)	Chloroform ($\varepsilon = 4.9$)	Ethanol ($\varepsilon = 24.55$)	Dimethlysulfoxide ($\varepsilon = 46.7$)	Water ($\varepsilon = 78.39$)
B3LYP	μ	1.9192	2.3558	2.5639	2.5878	2.6149
	α	34.314	42.400	45.728	46.1796	46.567
	Δα	102.107	123.864	127.045	131.430	132.089
	β	18.845	40.317	49.142	50.539	51.229
B3PW91	μ	1.9123	2.3469	2.5529	2.5776	2.6046
	α	33.943	41.962	45.258	45.6993	46.088
	Δα	101.432	123.125	129.823	130.665	131.353
	β	18.452	39.860	48.796	50.114	50.873

As can be seen from the Table 3, all the calculated values of the molecule were raised with the polarity of the solvent. Also, the values of the title compound were decreased with the high levels of theory. The polarizabilities and first hyperpolarizability are reported in terms of atomic units (a.u.) and the calculated these values have been converted by using 1 a.u = 0.1482×10^{-24} electrostatic unit (esu) for α and 1 a.u = 8.6393×10^{-33} esu for β. The calculated values of β are 18.845 and 18.452×10^{-30} esu for the B3LYP and B3PW91 methods, respectively. It was expected that the high values of β were obtained due to the low HOMO-LUMO gap. These values of the title compound are greater than thevalues of the urea (μ=1.5256 Debye and $\beta = 0.7803 \times 10^{-30}$ esu). The β values of the molecule is about 24.15 times for the B3LYP, 23.64 times bigger for the B3PW91 for the reference magnitude of urea [54]. The

handled first hyperpolarizability of the molecule show thatit may be possible a good applicant in the development of NLO materials.

3.4. Molecular electrostatic potential

MEP is a useful method for describing of the structure activity, hydrogen bonds and reactivity of molecule behaviors. Being a real physical property V(r) can be determined experimentally by diffraction or by computational methods [55]. To predict reactive sites for electrophilic and nucleophilic features for the investigated molecule, the MEP map was computed. The color code of these maps is in the range between -4.723 a.u. (dark red) +4.723 a.u. (dark blue) in the title compound. The negative sites of the MEP were related to electrophilic reactivity and the positive sites to nucleophilic reactivity (Figure 5).

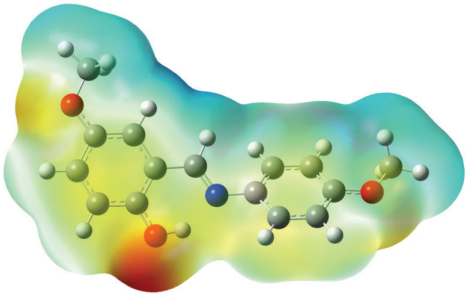

Figure 5. *Molecular electrostatic potential map calculated at B3LYP/6-311+G(d,p) level.*

As can be seen in figure, there are several possible sites of electrophilic attack. Negative electrostatic potential sites are mainly localized over the O1, O2 and N1 atoms, and then V(r) values are -0.040, -0.046 and -0.043 a.u, respectively. However, positive electrostatic potential sites are localized on the C-H atoms, and then maxsimum V(r) value is +0.025 for H2 atom. In addition,

The MEP method is the most suited one for describing sites for intra- and intermolecular interactions [56]. The MEP map supported that the existence of the O2-H2… N1 interaction.

3.5. Mulliken population analysis and natural population analysis

The Mulliken charge plays an important role in the application of quantum chemical calculations to molecular systems. It affects dipole moment, polarizability, electronic structure and more properties of the molecular system [57]. The natural population analysis (NPA) [58] and Mulliken atomic charges of the molecule were computed. According to the results, the negative charge is delocalized in oxygen and carbon atoms. The positive charge is observed for N and C-H atoms. The intramolecular charge transfer is revealed in the Mulliken charge analysis through the calculated charges of H2 (0.441 e) and O2 (-0.307 e) for the B3LYP; H2 (0.478 e) and O2 (-0.678 e) for the B3PW91 method. The atomic charges results are good agreement with the MEP map of the title compound. MEP and Mulliken charges analysis can be use for interpreting and predicting the reactive behavior of a wide variety of chemical systems in both electrophilic and nucleophilic reactions [59].

3.6. Thermodynamic properties

The thermodynamic fparameters such as enthalpy (H_m^0), entropy (S_m^0), heat capacity ($C_{p,m}^0$), thermal energy (E) and their component were computed at constant pressure (by changing temperature) and temperature (by changing pressure) in gas phase with B3LYP/6-311G+(d,p) level of theory. The thermodynamic functions were calculated at different tempera-

tures and pressure going from 100.00 to 500.00 K, and these functions were given in the Table 4.

Table 4. *Thermodynamic properties at different temperatures and pressure at the B3LYP and B3PW91 methods with the 6-311++G(d,p) level for the title compound.*

	T(K)	H_m^0 (kcal/mol)	$C_{p,m}^0$(cal/mol K)	S_m^0 (cal/mol K)		
	100	1.5976	26.251	85.998	***P(atm)=1***	134.306
	150	3.4519	35.996	99.294	***1.5***	133.502
	200	5.5955	45.793	11.558	***2***	132.927
	250	8.2341	55.809	123.293	***2.5***	132.486
B3LYP	***298.150***	***11.2512***	***65.542***	***134.304***		
	300	11.3767	65.914	134.724	***3***	132.122
	350	15.0206	75.800	145.939	***3.5***	131.809
	400	19.1465	85.173	156.942	***4***	131.560
	450	23.7248	95.850	167.720	***4.5***	131.319
	500	28.7179	101.759	178.233	***5***	131.105
	100	1.7858	26.116	85.744	***1***	133.899
	150	3.7858	36.116	85.741	***1.5***	133.092
	200	5.5729	45.664	111.215	***2***	132.524
	250	8.2040	55.646	122.925	***2.5***	132.077
B3PW91	**298.150**	***11.2123***	***65.341***	***133.905***		
	300	11.3378	65.712	134.316	***3***	131.717
	350	14.9704	75.563	145.498	***3.5***	131.407
	400	19.0844	84.913	156.468	***4***	130.514
	450	23.6489	93.576	165.213	***4.5***	130.911
	500	28.6276	101.480	177.689	***5***	130.704

The Table 4 shows that the standard thermodynamic functions increase with increasing temperature, due to the intensities of molecular vibration increase. It has been shown that the S_m^0 increases otherwise the H_m^0 and $C_{p,m}^0$ remain stable, when the pressure is increased at 298.15 K. According to Boyle Law, the volume and pressure of a gas are inversely related [60].

B3LYP;

H_m^o = -39043+ 0.0109 T + 9.47245 x 10^{-5} T^2 (R^2=0.99998)

$C_{p,m}^0$ = 4.35302 + 0.21774 T – 4.04866 x 10^{-5} T^2 (R^2=0.99872)

S_m^0 = 60.20684 + 0.26819 T – 6.496775 x 10^{-5} T^2 (R^2=0.99993)

B3PW91;

H_m^o = 0.10633 + 0.00815 T -9.79427 x 10^{-5} T^2 (R^2=0.99982)

$C_{p,m}^0$ = 4.32276 + 0.21875 T – 4.66659 x 10^{-5} T^2 (R^2=0.99965)

S_m^0 = 51.17373 + 0.31029 T +9.0065 x 10^{-5} T^2 (R^2=0.9819)

The obtained values may be useful in the further studies on the title compound.

4. Conclusions

In a previously study, the X-ray single-crystal analysis of 3-Methoxy-2-[(E)-(4-

methoxyphenyl)-iminomethyl]phenol, $C_{15}H_{15}NO_3$, had been studied. The aim of this current study was to detrmine the title compound electronic and structure properties of the Schiff base compound using B3LYP and B3PW91 methods with the 6-311++G(d,p) polarized and diffused basis set. The comparison between the theoretical and experimental results demonstrated that the B3LYP method results are in good agreement with the experimental data. The molecular energy surface scans selected torsion angle are performed by using the B3LYP/6-311++G(d,p) level of theoretical approximation for the molecule. The energy of the most stable conformation is 0.0702738 Hartree. So,

we expect this study will be beneficial for the design and composes of new materials like molecule further time.

Acknowledgement

I'm greatly thankful for the considerable contributions of my dear advisor Prof. Dr. Şamil Işık (pass away, may god bless his soul..)

REFERENCES

[1] M.D. Cohen, G.M.J. Schmidt, S. Flavian, J. Chem. Soc. 2041 (1964).

[2] S. Kumar, D. Dhar, P.N. Saxena, J. Sci. Ind. Res. **68** 181–187 (2009).

[3] D. Barton, W.D. Ollis, Comprehensive Organic Chemistry, (Pergamon, Oxford, 1979).

[4] R.W. Layer, Chem. Rew **63** 489-510 (1963).

[5] C.K. Ingold, Structure and Mechanism in Organic Chemistry, 2nd Ithaca, Cornell Universiy Press, 1969.

[6] Taggi, A. E., Hafez, A. M., Wack, H., Young, B., Ferraris, D., Lectka, T. The development of the first catalyzed reaction of ketenes and imines: catalytic, asymmetric synthesis of β-lactams. Journal of the American Chemical Society (2002), 124 (23), 6626-6635.

[7] G. Özdemir Tarı, Ş. Işık, Ramazan Özkan, A. Alaman Ağar, Acta Cryst. E67 (2011) o343–o344.

[8] Ç. Albayrak, B. Koşar, S. Demir, M. Odabaşoğlu, O. Büyükgüngör, J. Mol. Struct. 963 (2010) 211.

[9] H. Tanak, F. Erşahin, Y. Koysal, E. Ağar, Ş. Işık, M. Yavuz, J. Mol. Model. 15 (2009) 1281–1290.

[10] O. Şahin, Ç. Albayrak, M. Odabaşoğlu, O. Büyükgüngör, Acta Cryst. E61 (2005) o2859–o2861.

[11] G. Özdemir Tarı, H. Tanak, M. Macit, F. Erşahin, Ş. Işık, Acta Cryst. E66 (2010) o85.

[12] A. Trzesowska-Kruszynska, Stuct. Chem. 21 (2010) 131.

[13] Petek H, Albayrak Ç, Ağar E, Kalkan H. (*Z*)-6-[(2-Fluorophenyliminio)methylene]-2,3-dihydroxyphenolate. Acta Crystallographica Section E Structure Reports Online. 2006; 62: 3685.

[14] W. Koch, M.C. Holthausen, A Chemist's Guide to Density Functional Theory, second ed., WILEY/VCH Verlag GmbH, Weinheim, 2001.

[15] G. Özdemir Tarı, Ş. Işık, R. Özkan, A. Alaman Ağar, Acta Cryst. E**67** o343-o344 (2011).

[16] A.D. Becke, J. Chem. Phys. 98 (2009) 5648.

[17] C. Lee, W.T. Yang, R.G. Parr, Phys. Rev. B 37 (1988) 785.

[18] A.D. Becke, Phys. Rev. A 38 (1988) 3098.

[19] J.P. Perdew, J.A. Chevary, S.H. Vosko, K.A. Jackson, M.R. Pederson, D.J. Singh, C. Fiolhais, Phys. Rev. B 48 (1993) 4978.

[20] J.P. Perdew, K. Burke, Y. Wang, Phys. Rev. B **54** 16533 (1996).

[21] M.J. Frisch, G.W. Trucks, H.B. Schlegel, G.E. Scuseria, M.A. Robb, J.R. Cheeseman, J.A. Montgomery Jr., T. Vreven, K.N. Kudin, J.C. Burant, J.M. Millam, S.S. Iyengar, J. Tomasi, V. Barone, B. Mennucci, M. Cossi, G. Scalmani, N. Rega, G.A. Petersson, H. Nakatsuji, M. Hada, M. Ehara, K. Toyota, R. Fukuda, J. Hasegawa, M. Ishida, T. Nakajima, Y. Honda, O. Kitao, H. Nakai, M. Klene, X. Li, J.E. Knox, H.P. Hratchian, J.B. Cross, V. Bakken, C. Adamo, J. Jaramillo, R. Gomperts, R.E. Stratmann, O. Yazyev, A.J. Austin, R. Cammi, C. Pomelli, J.W. Ochterski, P.Y. Ayala, K. Morokuma, G.A. Voth, P. Salvador, J.J. Dannenberg, V.G. Zakrzewski, S. Dapprich, A.D. Daniels, M.C. Strain, O. Farkas, D.K. Malick, A.D. Rabuck, K. Raghavachari, J.B. Foresman, J.V. Ortiz, Q. Cui, A.G. Baboul, S. Clifford, J. Cioslowski, B.B. Stefanov, G. Liu, A. Liashenko, P. Piskorz, I. Komaromi, R.L. Martin, D.J. Fox, T. Keith, M.A. Al- Laham, C.Y. Peng, A. Nanayakkara, M. Challacombe, P.M.W. Gill, B. Johnson, W. Chen, M.W. Wong, C. Gonzalez, J.A. Pople, Gaussian 03, Revision E.01, Gaussian, Inc., Wallingford CT, 2004.

[22] R. Dennigton II, T. Keith, J. Millam, GaussView, Version 4.1.2, Semichem Inc.,Shawnee Mission, KS, 2007.

[23] E. Runge, E.K.U. Gross, Phys. Rev. Lett. **52** 997 (1984).

[24] R.E. Stratmann, G.E. Scuseria, M.J. Frisch, J. Chem. Phys. **109** 8218 (1988).

[25] E. Ermiş, Journal of Mol. Struct. **1156** 91-104 (2018).

[26] S. Uzun,Z. Esen,, E. Koç, N. C. Usta, M. Ceylan, Journal of Mol. Struct. **1178** 450-457 (2019).

[27] A. Eşme, S. G. Sağdınç, Journal of Mol. Struct. **1075** 264-278 (2014).

[28] A. Eşme, S. g. Sağdınç, Spectrochim. Acta Part A **188** 443-455 (2018).

[29] Minkin VI, Glukhovtsev M. N. Simkin BY Aromacity and Antiaromacity (Wiley, Newyork, 1994).

[30] J. Kruszewski , T. M. Krygowski, Tetrahedron Lett. **13** 3839-3842 (1972).

[31] T. M. Krygowski, J. Chem. Inf. Comput. Sci. **33** 70-78 (1993).

[32] A. Filarowski, A. Koll, T. Glowiak, J. Chem Soc. Perkin trans. **2** 835-842 (2002).

[33] A. Filarowski, A. Kochel, M. Kluba, F. S. Kamounah, J. Phys. Org. Chem. **21** 939-944 (2008).

[34] Etter, M. C., MacDonald, J. C. & Bernstein, J. Acta Cryst. B**46**, 256–262 (1990).

[35] Bernstein, J., Davies, R. E., Shimoni, L. & Chang, N.-L.. Angew. Chem. Int. Ed. Engl. **34**, 1555–1573. (1995)

[36] F.F. Jian, P.S. Zhao, Z.S. Bai, L. Zhang, Struct. Chem. **16** 635 (2005).

[37] I. Fleming, Frontier Orbitals and Organic Chemical Reactions, (Wiley, London, 1976).

[38] R.G. Pearson, J. Chem. Sci. **117(5)** 369-377 (2005).

[39] K. B. Benzon, H. T. Varghese, C. Yohannan Panicker, K. Pradhan, B. K. Tiwary, A. K. Nanda, C. V. Alsenoy, Spectrochim. Acta A **146** 307-322 (2015).

[40] Z. Demircioğlu, Ç.A. Kaştaş¸ O. Büyükgüngör, Spectrochim. Acta A **139** (2015) 539-548.

[41] H. Tanak, A. A. Ağar, O. Büyükgüngör, Spectrochim. Acta Part A **118** 672-682 (2014).

[42] A. A. Ağar, M. Yavuz, H. Tanak, Mol. Phys. **108** 1759-1722 (2010).

[43] B. Koşar, Ç. Albayrak, Spectrochim. Acta Part A **78** 160-167 (2011).

[44] U. Ceylan, G. Özdemir Tarı, H. Gökce, E. Ağar, Journal of Mol. Struct. **1110** 1-10 (2016).

[45] Y. Bingöl Alpaslan, H. Gökce, G. Alpaslan, M. Macit, Journal of Mol. Struct. **1097** 171-180 (2015).

[46] A. Soltani, F. Ghari, A. D. Khalaji, E. T. Lemeski, K. Fejfarova, M. Dusek, M. Shikhi, Spectrochim. Acta Part A **139** 271-278 (2015).

[47] G. Özdemir Tarı, S. Gümüş, E. Ağar, Spectrochim. Acta Part A **141** 119-127 (2015).

[48] M. Jalali-Heravi, A.A. Khandar, I. Sheikshoaire, Spectrochim. Acta A **55** 2537 (1999).

[49] J.F. Nicoud, R.J. Twieg, in: D.S. Chemla, J. Zyss (Eds.), Nonlinear Optical Properties of Organic Molecules and Crystals, vol. 1, Academic Press, Newyork, 1987, p. 277. Chap. II-3.

[50] M. Jalali-Heravi, A.A. Khandar, I. Sheikshoaire, Spectrochim. Acta A 56 (2000) 1575.

[51] Y. R. Shen, The Principles of Nonlinear Optics, (Wiley, New York, 1984).

[52] Y. Q. Ge, Y. Xia, F. Wei, W. L. Dong, B. X. Zhao, Acta Cryst. E63 (2007) o1186-o1187.

[53] M.G. Papadopoulos, A.J. Sadlej, J. Leszscynski, Non-linear Optical Properties of Matter Publication Series Challenges and Advances in Computational Chemistry and Physics, vol. 1, 8Springer, Berlin, Germany, 2006).

[54] S. Ramalingam, S. Periandy, M. Karabacak, N. Karthikeyan, Spectrochim. Acta A **104** 337-351 (2013).

[55] P. Politzer, D. G. Truhlar (Eds.), Chemical Application of Atomic and Molecular Electrostatic Potentials, (Plenum, New York, 1981).

[56] P. Politzer, M.C. Concha, J.S. Murray, Int. J. Quantum Chem. **80** 184 (2000).

[57] M. Govindarajan, M. Karabacak, Spectrochim. Acta Part A **96** 421-435 (2012).

[58] R. S. Mulliken, J. Chem. Phys. **23**, 1883-1840 (1955).

[59] Z. Demircioğlu, Ç. Albayrak Kaştaş, O. Büyükgüngör, Journal of Molecular Structure **1091** 183-195 (2015).

[60] J.B. West, J. Appl. Physiol. **87** 1543-1545 (1999).

SWELLING AND DEGRADATION BEHAVIORS OF MULTILAYER GELATIN-CHITOSAN HYDROGEL SYSTEMS

Mehlika PULAT[1]

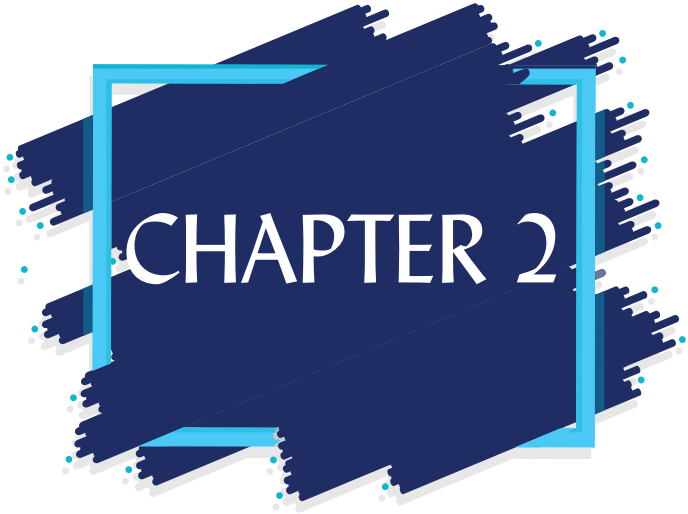

1 Department of Chemistry, Faculty of Sciences, Gazi University, Teknikokullar, Ankara, Turkey, mpulat@gazi.edu.tr

SWELLING AND DEGRADATION BEHAVIORS OF MULTILAYER GELATIN-CHITOSAN HYDROGEL SYSTEMS

Mehlika PULAT[1]

INTRODUCTION

Hydrogels are three-dimensionally structure consisting of crosslinked polymer chains. They can absorb and retain considerable amounts of water. The hydrophilic property is due to presence of chemical groups in molecular structure such as -COOH, –OH, -NH2, -CONH2, -SO3H and others. Hydrogels have been extensively studied and used for a large number of applications in medicine, such as controlled drug release matrices, enzyme and yeast cell immobilization, and blood-contact applications [Elvira, C et al., 2002; Pulat M and Asıl D, 2009]. They are also very useful materials for agricultural and horticultural applications [Pulat M & Yoltay N, 2016].

Most of the synthetic polymers used to prepare hydrogels causes some problems because of their long degradation times and degradation products. Natural polymers are a good choice to overcome this issue [Pulat M & Akalın G.O., 2013].

Gelatin is a mixture of peptides and proteins produced by partial hydrolysis of collagen extracted from the skin, bones, and connective tissues of animals. It is obtained by thermal denaturation or physical and chemical degradation of collagen [Kushibiki T. et al., 2003; Gilsenan P. & Ross-Murphy S., 2001] (Figure 1). Gelatin is a biodegradable natural polymer with extensive industrial, pharmaceutical, and biomedical uses that has been employed for coatings

1 Department of Chemistry, Faculty of Sciences, Gazi University, Teknikokullar, Ankara, Turkey, mpulat@gazi.edu.tr

and microencapsulating various drugs, and for preparing biodegradable hydrogels [Pulat M. & Akalın G.O., 2013]. Since it is soluble in aqueous solutions, the materials for long-term applications must be submitted to crosslinking, which improves both thermal and mechanical stability of gelatin [Bigi A. et al., 2001].

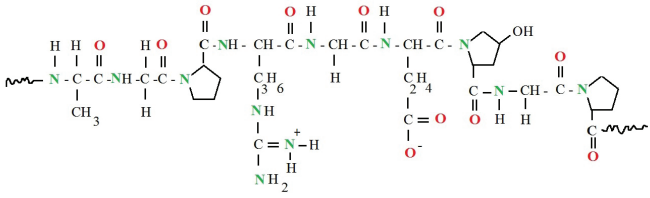

Figure 1. *Molecular formula of gelatin*

Chitosan (Cs) is a biodegradable cationic amino polysaccharide obtained through alkaline deacetylation of chitin (Figure 2). Chitin is the second most important natural polymer in the world. The main sources exploited are two marine crustaceans, shrimp and crabs.

Cs stands out by some unique combination of favorable biological properties such as nontoxicity, biocompatibility, biodegradability, along with muco-adhesive, bacteriostatic, and wound-healing properties [Berger, J. et al., 2004; , El-Sherbiny, et al., 2005]. In addition, this cationic biopolymer has been reported to improve transport across biological barriers [Kotze´, A. F. Et al., 1999]. Finally, Cs is very abundant and its production is both environmentally safe and of low cost.

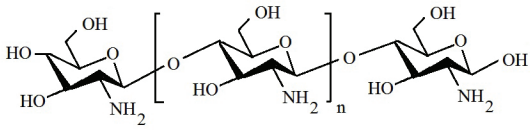

Figure 2. *Molecular formula of Cs*

From a biomedical point of view, Cs has demonstrated high activity as wound healing activators or accelerators, and now is used in human and veterinary medications. Several researchers have reported on the mechanism of the activation of wound healing considering the activation of polymorpho nuclear cells, protective effects against microorganisms, or the promotion of granulocyte tissue formation with angiogenesis.

The hydrophilicity of Cs, due to the presence of amine and hydroxyl functional groups in its repeat unit, makes the polymer soluble in dilute acidic solutions and yields to a rubbery hydrogel in water. The propensity of Cs to absorb water and swell into a soft rubbery material makes it a good matrix material for incorporating hydrophilic drugs [Pulat M. et al., 2011].

The aim of this study is to prepare a series of multilayer hydrogel systems by using gelatin and Cs polymers. The effect of composition of the hydrogels on swelling and degradation behaviors will also be investigated.

EXPERIMENTAL

Preparation of hydrogels

A series of three layers hydrogels were prepared using gelatin (Fluka, Type B, 280-Bloom) and Cs (Aldrich) by ionotropic gelation method [Nitsae M. et al., 2016]. Hydrogel samples were composed from one Cs phase between two gelatin stratums. This structure resembles two layer sandwich models. All of the gelatin layers (G) were formed by crosslinking of gelatin with GA (25% of solution, Aldrich). In spite of this, only half of hydrogels were prepared by using crosslinked Cs. Other half was formed with un-crosslinked Cs phase.

Firstly, 1% of Cs in 5% of acetic acid (Merck) and 10% of aqueous gelatin solutions were prepared. Gelatin solutions were quickly mixed with GA solution and poured into plastic square box. After 1 hour, once gelatin layer became solid Cs solution was flowed onto gelatin layer. Thirdly, the crosslinked gelatin stratum was formed at the top of the bilayer structure, similar to the bottom layer. Each layers were kept waiting for one hour. After three stratums were formed, the boxes were left in room conditions for 24 hours. Four samples were formed by crosslinking of Cs with GA. Totally; eight types of three layers hydrogels were obtained. The components and amounts of the hydrogels were presented in Table 1.

Table 1 *The amount of components and preparation conditions of the hydrogels*

Components / Hydrogels	G (mL)	Cs (mL)	G (mL)	GA	(X, mL)	
G-[1C]-G	5.0	1.0	5.0	0.2	0	0.2
G-[2C]-G	5.0	2.0	5.0	0.2	0	0.2
G-[3C]-G	5.0	3.0	5.0	0.2	0	0.2
G-[4C]-G	5.0	4.0	5.0	0.2	0	0.2
G-[2CX]-G	5.0	2.0	5.0	0.2	0.5	0.2
G-[3CX]-G	5.0	3.0	5.0	0.2	0.7	0.2
G-[4CX]-G	5.0	4.0	5.0	0.2	1.0	0.2
G-[5CX]-G	5.0	5.0	5.0	0.2	1.2	0.2

The formed multilayer hydrogels were displaced from plastic square boxes and immersed in distilled water in order to remove unparticipated ingredients. After purification, the samples were cut as 1cm^2 and dried in oven at 40 °C. The schematic representation was given in Figure 3.

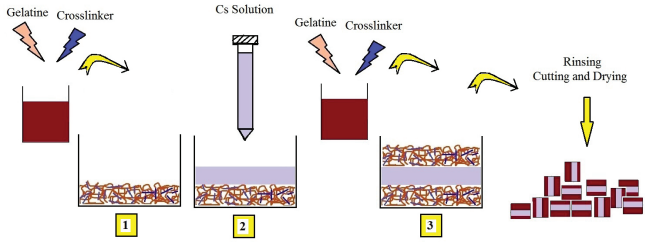

Figure 3. *The schematic representation for the formation of multilayer hydrogels*

Swelling studies

Swelling tests of cubic hydrogel were gravimetrically carried out in three steps [Pulat M. & Eksi H, 2006]. In the first step, dried discs were left to swell in Britton–Robinson Tampon (BRT) (Riedel-de Haen) solution (pH = 7.0) at 30ºC. Swollen hydrogels removed from the swelling medium at regular intervals were dried superficially with filter paper, weighed, and placed into the same bath. The measurements were performed until a constant weight was reached for each sample. The percentage swelling (S%) values were calculated from the following equation:

$$\text{Swelling (S\%)} = \frac{Ww - Wd}{Wd} \times 100 \qquad (1)$$

where Ww is the wet weight of the sample and Wd is the dry weight of the sample before swelling. The incubation times for all gels were approximately 24 h.

In the second step, the dried hydrogel samples were swollen in BRT (pH = 7.0) solutions at different temperatures ranging from 4 to 60ºC to investigate the effect of temperature on swelling behaviors. At the end of 24 h, the swollen cubes were removed from the swelling

medium, dried superficially with filter paper, and weighed. S% values were calculated using Equation 1.

In the last step, the dried cubic hydrogels were swollen in different BRT solutions at various pH values between 1 and 11 to investigate the effect of pH on the swelling behaviors. Temperature and swelling time were kept constant (30ºC and 24 h, respectively). The swollen samples were removed from the swelling medium, dried superficially with filter paper, and weighed. S% values were calculated using Equation 1.

All measurements were performed in triplicate.

Degradation test

Degradation tests of the hydrogel were carried out at pH 7.0 and 30°C [Vashist, A. Et al., 2012; Pulat, M. & Özgündüz, H.I., 2014]. Dried hydrogel cubes were left to swell in BRB solution. Swollen gels were removed from the swelling bath at the end of 48 h, dried superficially with filter paper, and weighed. This mass (Mm) was recorded as the maximum swollen state of hydrogels. Then they were placed into the same bath and weighing was continued at regular intervals until the hydrogels completely degraded. The degradations (%) were determined using the following formula:

$$\text{Degradation (\%)} = \frac{Mm - Mt}{Mm} \times 100 \qquad (2)$$

where Mm is the weight of hydrogel at the maximum swollen stage and Mt is the weight of hydrogel at time t. All measurements were performed in triplicate.

RESULTS AND DISCUSSION

Swelling behaviors of the hydrogels

Figure 4 and Figure 5 represent the variation of S% values with time at pH = 7.0 and 30°C. The date belongs to a pure gelatin hydrogels were also placed for cooperation. For all samples, S% increased with time initially and then remained constant at close to 20 h.

In general, swelling behaviors of the hydrogels depend on composition, monomer ratio, ionic charge content, polymerization route, type and density of cross-linker, and so forth [El-Sherbiny, et al., 2005]. In this study, the sandwich types of hydrogels were prepared by changing the composition of inner phase. The first group was obtained by varying the Cs volume that causes a thickness gradient. The second group was prepared by crosslinking of Cs at different ratio.

From Figure 4, it is seen that the swelling percentages decreased while the Cs layer became more thickness. S% values were determined to be 201% for the most swollen hydrogel G-[1C]-G, and 138% for the least swollen hydrogel G-[4C]-G. This result could be explained via hydrophilic properties of the components. As gelatin is more hydrophilic than Cs, increasing amount of Cs caused the decreased swelling values [Pulat M. & Eksi H, 2006]. It is clearly seen that the most swollen sample was the pure gelatin hydrogel.

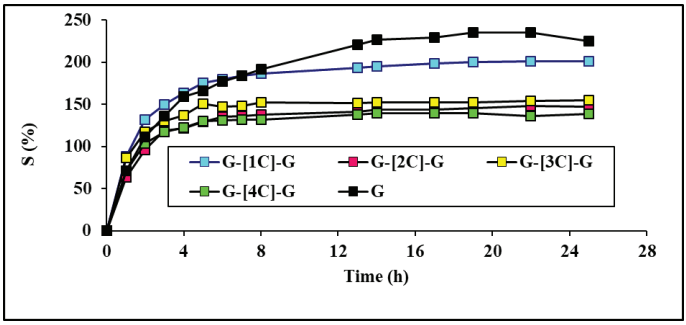

Figure 4. *The variation of S% values of the hydrogels including un-crosslinked Cs layer with time at pH =7.0 and 30 ºC.*

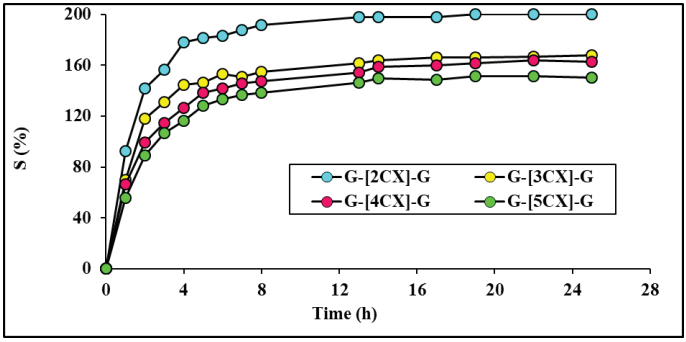

Figure 5. *The variation of S% values of the hydrogels including crosslinked Cs layer with time at pH =7.0 and 30 ºC.*

From Figure 5, it is seen that the swelling percentages decreased while the crosslinking degree of Cs was increased. S% values were determined to be 200% for the most swollen hydrogel G-[2CX]-G, and 151% for the least swollen hydrogel G-[5CX]-G. Similar to the firs group, the increased amount of Cs caused the less swelling values.

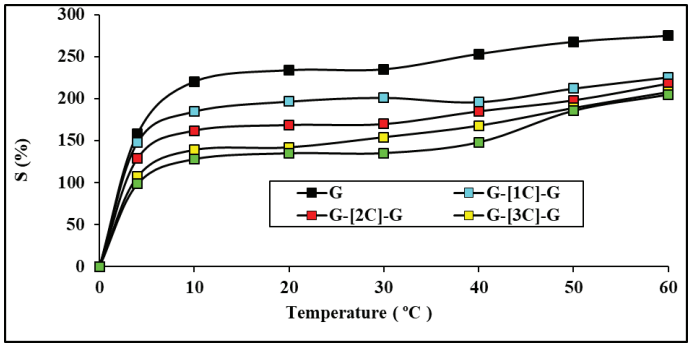

Figure 6. *The variation of S% values of the hydrogels including uncrosslinked Cs layer with temperature at pH = 7.0 and 24 h.*

Figure 6 and Figure 7 represent the variation of S% values with temperature at pH = 7.0 and 24 h. As seen from these figures, swelling percentages slightly vary with temperatures. It is known that swelling of gelatin and Cs hydrogels positively depends on temperature. As the temperature increases, thermal mobility of the polymer chains increases and H-bonds were broken, and hydrogels can easily swell [Katona, H. et al., 1991; Xiao, X.C. et al., 2005].

From Figure 6, it is seen that the swelling percentages decreased while the Cs layer became more thickness. From Figure 7, it is determined that the swelling percentages decreased while the crosslinking degree of Cs was increased and the most swollen hydrogel is G-[2CX]-G.

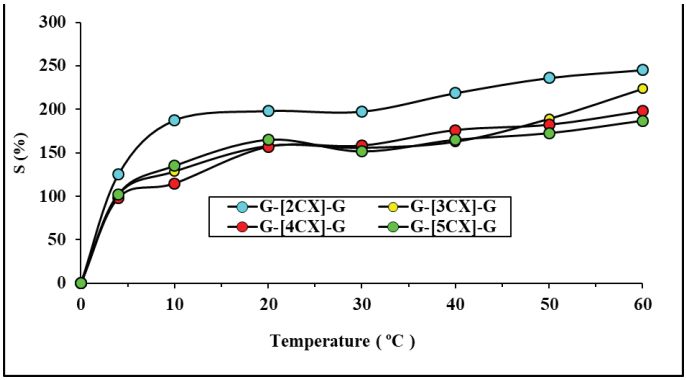

Figure 7. *The variation of S% values of the hydrogels including crosslinked Cs layer with temperature at pH =7.0 and 24 h.*

Figure 8 and Figure 9 represent the variation of S% values with pH at 30°C and 24 h.

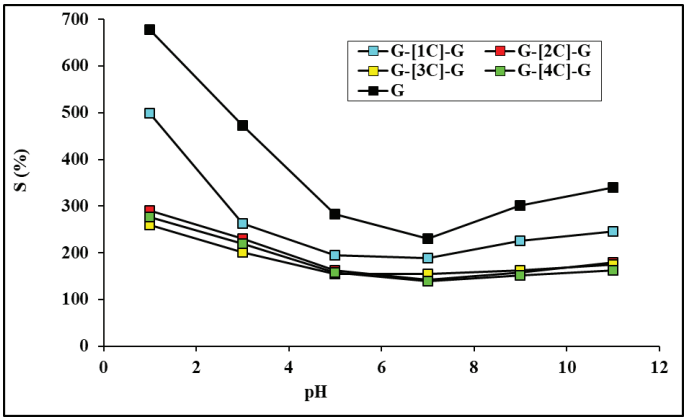

Figure 8. *The variation of S% values of the hydrogels including un-crosslinked Cs layer with pH at 30 ºC and 24 h.*

As seen from these figures, S% values present U-type variation. The hydrogels swell both in acidic and basic mediums. The minimum swelling values were obtained near pH=4-5. As is known, gelatin is a weak polyelectrolyte, so its net charge is strongly dependent on pH. The nominal pI of gelatin is 4.9 [Rafieian, F. et al., 2015]. At this pH

there is ought to be an exact balance of positive and negatively charged sites on gelatin network. Above pI the gelatin network bears a net negatively charged backbone yielding an anionic gel [Boral, S et al., 2006; Deiber, J.A. et al., 2009]. The effect of pH on the swelling behaviors of gelatin components might be reduced by Cs content.

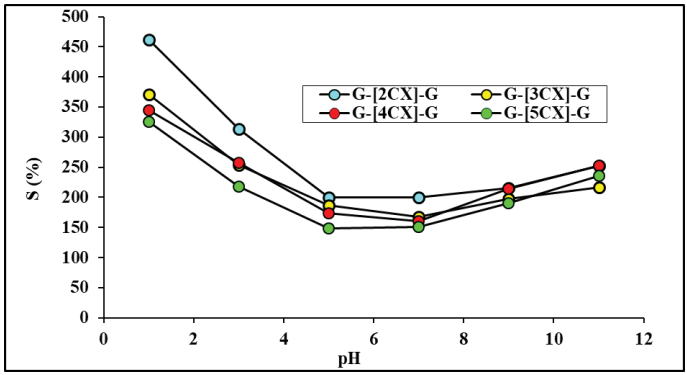

Figure 9. *The variation of S% values of the hydrogels including crosslinked Cs layer with pH at 30 ºC and 24 h.*

Degradation behaviors of the hydrogels

As gelatin and Cs are natural and biodegradable polymers, degradation behaviors of the hydrogels prepared in this study are very important. Figure 10 and Figure 11 show the degradation behaviors of these hydrogels at 30°C and pH 7.0.

As seen from Figure 10, the thickness of Cs layer prolong the degradation time of hydrogels. G-[4C]-G hydrogel exhibits the slowest degradation, close to three mounts.

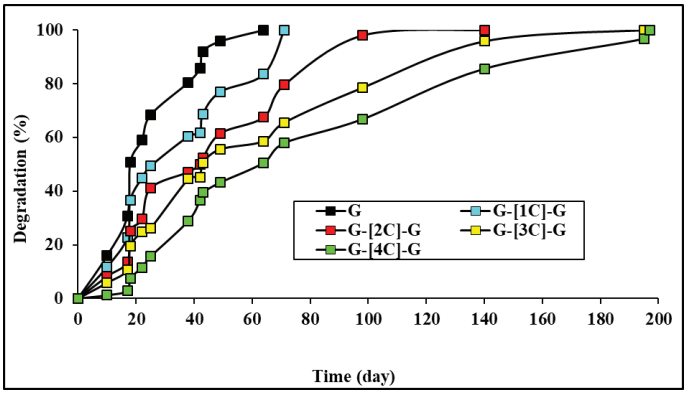

Figure 10. *Degradation of the hydrogels including uncrosslinked Cs layer at 30 ºC and 24 h.*

Similar profile was observed for the hydrogels including crosslinked Cs layer. The fastest degraded structure is G-[2CX]-G hydrogel. While the crosslinked Cs layer became ticker, degradation time increased up to 140 days.

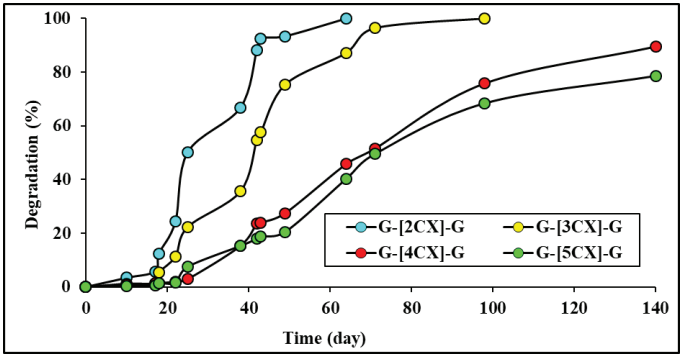

Figure 11. *Degradation of the hydrogels including crosslinked Cs layer at 30ºC and 24 h.*

Conclusion

In this study a series of multilayer hydrogel systems were produced using gelatin and Cs. These polymers are chosen because of their biodegradable and biocompatible properties. The structures were prepared in sandwich type which contains Cs phase between two gelatin layers. Gelatin stratums were obtained by crosslinking with *GA.* Half of the samples were prepared by crosslinking of Cs phase with GA. Swelling tests of all hydrogel samples were gravimetrically carried out and swelling percentages were calculated. It is found that the swelling values decreased while the thickness of Cs layer increased. The swelling values of all hydrogels were found to be in between 138% and 200%. Temperature affect on swelling was also investigated and it is found that the swelling percentages slightly vary with temperatures. The degradation tests show that the thickness of Cs layer prolongs the degradation time of hydrogels. While the Cs layer became ticker, the longer degradation times were obtained up to 140 days. It can be concluded that the multilayer hydrogel structures produced in this study is much promising in utilizing a natural resource like gelatin in the production of matrix material, which could significantly reduce the production costs and offer a quite environmental friendly alternative technique.

REFERENCES

Bigi A., Cojazzi G., Panzavolta S., Rubini K., Roveri N. (2001). Mechanical and thermal properties of gelatin films at different degrees of glutaraldehyde crosslinking. *Biomaterials 22*, 763-768.

Berger, J.; Reist, M.; Mayer, J. M.; Felt, O.; Gurny, R. (2004). Europian Journal Pharma Biopharma, 57, 35.

Boral, S., Gupta, A.N., and Bohidar, H.B., (2006). Swelling and de-swelling kinetics of gelatin hydrogelsin ethanol–water marginal solvent. International Journal of Biological Macromolecules, 39:240–249.

Deiber, J.A., Ottone, M.L., Piaggio, M.V., and Peirotti, M.B. (2009) Characterization of cross-linked polyampholytic gelatin hydrogels through the rubber elasticity and thermodynamic swelling theories. Polymer, 50:6065–6075.

El-Sherbiny, I. M.; Lins, R. J.; Abdel-Bary, E. M.; Harding, D. R. K. (2005) Europian Polymer Journal, 41, 2584.

Elvira, C.; Mano, J. F.; SanRoman, J.; Reis, R. L. (2002). Starch-based biodegradable hydrogels with potential biomedical applications as drug delivery systems, *Biomaterials* 23, 1955-1966.

Gilsenan P, Ross-Murphy S. 2001. Shear creep of gelatin gels from mammalian and piscine collagens. *International Journal of Biological Macromolecules* 29: 53–61.

Katona, H., Maruyama, K., Sanui, K., Okano, T., and Sakuai, Y. (1991) Thermo-responsive swelling and drug release switching of interpenetrating polymer Networks composed of poly(acrylamide-co-butyl methacrylate) and poly (acrylic acid). *Journal of Controlled Release*, 16:215–227.

Kotze´, A. F.; Luesen, H. L.; Boer, A. G.; Verhoef, J. C.; Junginger, H. E. (1999). *European* Journal of Pharmaceutical Sciences, 7, 145.

Kushibiki T, Tomoshige R, Fukunaka Y, Kakemi M, Tabataa Y. (2003). In vivo release and gene expression of plasmid DNA by hydrogels of gelatin with different cationization extents. *Journal of Control Release* 90: 207–216.

Nitsae M., Madjid A., Hakim L. and Sabarudin A., (2016). Preparation of chitosan beads using trıpolyphosphate and ethylene glycol diglycıdyl ether as crosslinker for Cr(vı) adsorption. *Chemistry & Chemical Technology,* Vol. 10, No. 1., 105-113.

Pulat M., Asıl D. (2009). Fluconazole release through semi-ipn hydrogels based on chitosan, AA, and citraconic acid. *Journal of Applied Polymer Sciences. 113*, 2613-2619.

Pulat M., Yoltay N. (2016). Smart fertilizers: preparation and characterization of gelatin-based hydrogels for controlled release of MAP and AN fertilizers**,** *Agrochimica*, 60:4, 249-261.

Pulat M., Akalın G.O. (2013). Preparation and characterization of gelatin hydrogel support for immobilization of *C. Rugosa* Lipase, *Artificial Cells***,** *Nanomedicine*, and *Biotechnology, 41*, 145-151.

Pulat M, Tan N, Onurdag FK. (2011). Swelling Dynamics of IPN Hydrogels Including Acrylamide-Acrylic Acid-Chitosan and Evaluation of their Potential for Controlled Release of Piperacillin-Tazobactam, *Journal of Applied Polymer Science*, Vol. 120, 441–450.

Pulat M. and Eksi H. (2006). Determination of Swelling Behavior and Morphological Properties of Poly(acrylamide-co-itaconic acid) and Poly(acrylic acid-co-itaconic acid) Copolymeric Hydrogels, *Journal of Applied Polymer Science,* Vol. 102, 5994–5999.

Pulat, M. and Özgündüz, H.I. (2014) Swelling behavior and morphological properties of semi-IPN hydrogels based on ionic and non-ionic components. *Bio-Medical Materials and Engineering*, 24:1725–1733

Xiao, X.C., Chu, L.Y., Chen, W.M., and Zhu, J.H. (2005) Monodispersed thermo-responsive hydrogel microspheres with a volume phase transition driven by hydrogen bonding. Polymer, 46:3199–3209.

Rafieian, F., Keramat, J., and Shahedi, M. (2015) Physicochemical properties of gelatin extracted from chicken deboner residue. *Food Science and Technology*, 64:1370–1375.

Vashist, A., Gupta, Y.K., and Ahmad, S. (2012) Interpenetrating biopolymer network based hydrogels for an effective drug delivery system. *Carbohydrate Polymers*, 87:1433–1439.

POLLEN CHARACTERS OF BRASSICACEAE FROM TURKEY AND THEIR TAXONOMIC APPLICATIONS

Mehmet Cengiz KARAİSMAİLOĞLU[1]

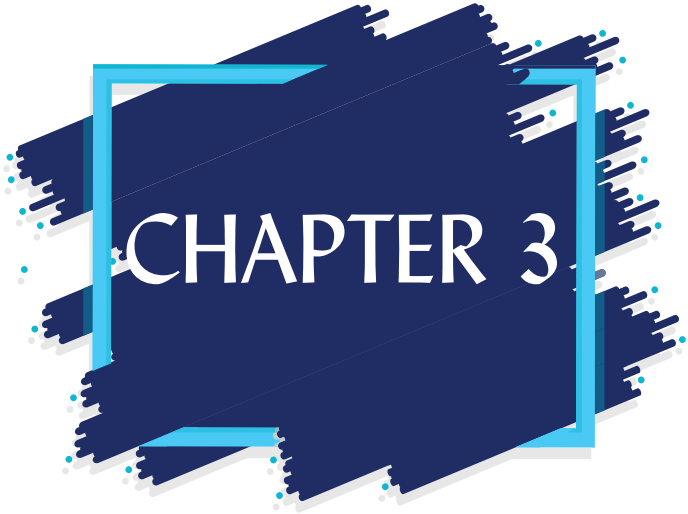

1 Department of Biology, Faculty of Arts and Sciences, Siirt University, Siirt, Turkey, cengiz.karaismailoglu@siirt.edu.tr

POLLEN CHARACTERS OF BRASSICACEAE FROM TURKEY AND THEIR TAXONOMIC APPLICATIONS

Mehmet Cengiz KARAİSMAİLOĞLU[1]

1. INTRODUCTION

Brassicaceae is a significant plant family due to commercial and technical practices in some scientific fields using taxa such as *Arabidopsis* Heynh. and *Brassica* L. (Al-Shehbaz et al., 2006; Filiz et al., 2014). It comprises approximately 3980 species, 351 genera, and 52 tribes, and that number continually increases (Kiefer et al., 2014). In Turkey, the family Brassicaceae comprises 571 species with 65 subspecies, 24 varieties, and 690 taxa belonging to 91 genera (Al-Shehbaz et al., 2007; Guner et al., 2012).

It is unlikely to be able to clarify the evolutionary relationships among most of the taxa in Brassicaceae merely by studying the morphological characters, due to common convergence (Franzke et al., 2011; Karaismailoğlu and Erol, 2018 and 2019). Thus, it is necessary to use the taxa's extra characteristics, which allows the separation from each other taxa, to answer the taxonomic problems about closely related taxa.

Pollen morphological characteristics have been proven to be beneficial in solving taxonomic problems. Some studies including pollen features have assisted in systematical problems with some genera of Brassicaceae (Inceoglu and Karamustafa, 1977; Dogan and Inceoglu, 1990; Brochmann, 1992; Anchev and Deneva, 1997; Khalik et al., 2002; Khan, 2004; Pınar et al., 2009; Mutlu and Erik, 2012; Kızılpınar et al., 2012; Kaya et al., 2017;

1 Department of Biology, Faculty of Arts and Sciences, Siirt University, Siirt, Turkey, cengiz.karaismailoglu@siirt.edu.tr

Karaismailoğlu, 2017; Karaismailoğlu and Erol, 2019). However, there are no studies comparing the pollen properties of taxa belonging to the genera of the family.

2. Materials and Methods

The plant taxa were collected from native inhabitants in Turkey. The collection and locality information of the specimens are presented in Table 1. The specimens were stored in the Siirt University Fauna and Flora center (SUFAF) or in the M.C. Karaismailoğlu personal collection.

For micromorphological remarks of the pollen, the specimens were arranged for electron microscopy: they were covered on a stub with silver epoxy, mounted with gold, and observed using a JEOL Neoscope-5000 scanning electron microscope (Karaismailoğlu, 2015).

Pollen slides were studied by utilizing the Wodehouse (1935) method. Flower specimens from each taxon were fixed in Carnoy's solution. The flowers were removed from the solution and then the anthers, taken from ripe floral buds, were mounted with a glycerine-gelatine-liquid safranin mixture (Candan and Öztürk **Çalı**, 2015; Karaismailoğlu and Erol, 2019). The observations were performed with 50 or more pollens from 5 individuals.

The slides were examined using an Olympus CX21FS1 light microscope and photographed using Kameram Imaging Software. The used pollen terminology was in line with that of Faegri and Iversen (1989), Brochmann (1992), Punt et al. (2007), and Karaismailoğlu and Erol (2019)

The 12 palynological characteristics were selected to discriminate the 44 taxa from the family Brassicaceae (Table 2). The taxa were clustered according to the distinction

of the chosen characteristics usage the unweighted pair group method with arithmetic mean (UPGMA) clustering analysis method (Figure 4) (Mohammadi and Prasanna 2003). The ordination method was based on the principal component analysis (PCA) (Figure 5). All the calculations were made using MVSP software (Kovach, 2007).

Table 1. The studied taxa and their origins.

No.	Taxa	Location	Voucher
1	*Alliaria petiolata* (Bieb.) Cavara et Grande	Uşak, Banaz, 1500 m, 25.6.2016	Karaismailoğlu 291
2	*Alyssoides utriculata* (L.) Med. var. *utriculata*	Bursa, Uludağ, 1600–1650 m, 1.7.2016	Karaismailoğlu 293
3	**Alyssum haussknechtii* Boiss.	Bolu, Abant, 1680 m, 21.5.2016	Karaismailoğlu 247
4	*Alyssum murale* waldst. et kit. var. *murale*	Gümüşhane, Kürtün, 675 m, 13.7.2014	Karaismailoğlu 74b
5	*Alyssum parviflorum* Fisch. ex M. Bieb.	İstanbul, Büyükçekmece-Çatalca, 4 m, 8.7.2016	Karaismailoğlu 312
6	*Alyssum sibiricum* Willd.	Kütahya, Gediz, 1350 m, 24.6.2016	Karaismailoğlu 290
7	*Alyssum szowitsianum* Fisch. et Mey.	Gümüşhane, Ziga-na-Kürtün, 850 m, 27.3.2015	Karaismailoğlu 115b
8	*Arabis caucasica* subsp. *brevifolia* Cullen	Niğde, Çamardı, 2083 m, 12.6.2016	Karaismailoğlu 272
9	*Arabis caucasica* Willd. subsp. *caucasica*	Kütahya, Gediz, 1800 m, 23.6.2016	Karaismailoğlu 287
10	*Arabis sagittata* DC.	Kütahya, Gediz, 1400 m, 24.6.2016	Karaismailoğlu 288
11	**Aubrieta canescens* Bornm. subsp. *cilicica* Cullen	Nigde, Camardi, 2083 m, 12.6.2016	Karaismailoğlu 269
12	**Aubrieta canescens* Bornm. subsp. *canescens*	Konya, Beyşehir, 1850 m, 24.08.2013	Karaismailoğlu 24
13	*Aubrieta deltoidea* DC.	Trabzon, Caykara, 950 m, 27.5.2017	Karaismailoğlu 379
14	*Barbarea plantaginea* DC.	Kayseri, Gemerek, 1250 m, 14.8.2016	Karaismailoğlu 333

15	*Barbarea vulgaris* R. Br.	Bursa, Uludag, 1350 m, 2.7.2016	Karaismailoğlu 299
16	*Berteroa mutabilis* DC.	Kirklareli, Derekoy, 650 m, 7.6.2014	Karaismailoğlu 46
17	**Bornmuellera kiyakii* Z. Aytaç et A.Aksoy	Konya, Derebucak, 1500 m, 11.7.2016	Karaismailoglu 321
18	*Cakile maritima* Scop.	Balikesir, Bandirma, 30 m, 9.7.2016	Karaismailoglu 313
19	*Caleapina irregularis* Thell.	Kirklareli, Demirkoy-Balaban, 320 m, 14.3.2015	Karaismailoglu 107
20	*Camelina rumelica* Velen.	Corum-Iskilip, 1095 m, 3.5.2015	Karaismailoglu 147
21	*Cardamine bulbifera* Crantz	Agri, Patnos, 1650 m, 16.5.2015	Karaismailoglu 160
22	*Cardamine hirsuta* L.	Bursa, Uludag, 1650 m, 2.7.2016	Karaismailoğlu 302
23	*Cardamine impatiens* var. *pectinata* Trautv.	Bolu, Abant, 801 m, 30.4.2015	Karaismailoğlu 132b
24	*Cardamine lazica* Boiss. et Bal.	Artvin, Hopa, 350 m, 6.3.2015	Karaismailoğlu 100b
25	*Cardamine uliginosa* Bieb	Istanbul, Buyukce-kmece, 80–120 m, 6.7.2016	Karaismailoğlu 310
26	*Clypeola jonthlaspi* L.	Mersin, Mut, 900 m, 27.7.2012	Karaismailoğlu 11
27	*Conringia orientalis* (L.) Dumort.	Kutahya, Gediz, 850 m, 23.6.2016	Karaismailoğlu 283
28	*Draba bruniifo-lia* Stev. subsp. *olympica*	Kutahya, Gediz, 1200 m, 23.6.2016	Karaismailoğlu 285
29	*Draba verna* L.	Mugla, Marmaris, 490 m, 3.4.2015	Karaismailoğlu 122a
30	*Erysimum crassipes* Fisch. et Mey.	Osmaniye, Urun, 1204 m, 26.5.2015	Karaismailoğlu 180b
31	*Erysimum cuspida-tum* (Bieb.) DC.	Kutahya, Gediz, 1700 m, 23.6.2016	Karaismailoğlu 282
32	*Hesperis persica* Boiss.	Trabzon, Caykara, 1100 m, 11.7.2014	Karaismailoğlu 70a
33	*Iberis sempervirens* L.	Bolu, Abant, 1680 m, 21.5.2016	Karaismailoğlu 249

34	*Iberis spruneri* Jord.	Bursa, Uludag, 950 m, 3.7.2016	Karaismailoğlu 304
35	**Isatis arenaria* Azn.	Istanbul, Buyukce-kmece, 80-120 m, 6.7.2016	Karaismailoğlu 306
36	*Isatis glauca* Aucher ex Boiss. subsp. *glauca*	Erzurum, Askale, 1700 m, 24.8.2016	Karaismailoğlu 340a
37	*Lepidium draba* L.	Kastamonu, Tosya, 745 m, 30.4.2015	Karaismailoğlu 135
38	*Lepidium latifolium* L.	Konya, Cihanbeyli, 850 m, 11.7.2016	Karaismailoğlu 318
39	*Matthiola montana* Boiss.	Trabzon, Caykara, 1100 m, 11.7.2014	Karaismailoğlu 70b
40	*Nasturtium officinale* R. Br.	Kirklareli, Koru-koy-Derekoy, 506 m, 21.3.2015	Karaismailoğlu 114
41	*Rorippa amphibia* (L.) Bess.	Balikesir, Manyas, 50 m, 9.7.2016	Karaismailoğlu 315
42	*Rapistrum rugosum* (L.) All.	Kirklareli, Derekoy, 650 m, 7.6.2014	Karaismailoğlu 48
43	*Sinapis arvensis* L.	Samsun, Kavak, 766 m, 2.5.2015	Karaismailoğlu 140b
44	*Turritis laxa* (Sibth. et Sm.) Hayek	Hatay, Dortyol, 1600 m, 24.4.2016	Karaismailoğlu 239a

3. Results

The morphological features of the pollen from the studied taxa are presented in Table 2. Photographs of the pollen have been demonstrated in Figures 1–2. The pollen are typically radially isopolar and prolate (prolate, perprolate, or subprolate) or prolate-spheroidal with the polar axis (P) varying between 14.04 and 25.29 µm, and the equatorial axis (E) varying between 7.19 and 17.93 µm. The percentages of the different forms are as follows: 47.72% prolate, 13.63% subprolate, 31.82% perprolate, and 6.83% prolate-spheroidal. The pollen dimensions are the smallest in *Alyssum sibiricum* and *Iberis sempervirens*, and the largest in *Cakile maritima* and *Conringia orientalis*. The pollen outlines are oval or circular in equatorial view

and elliptical or triangular in polar view (amb) (Table 2 and Figures 1–3).

The aperture number of the studied pollen has ranged from 1 to 4. The most commonly observed aperture type is tricolpate. The other forms are viewed in some taxa: dicolpate in *Camelina rumelica*, *Conringia orientalis*, and *Lepidium latifolium*; monocolpate in *Clypeola jonthlaspi*; and tetracolpate in *Barbarea plantaginea*. Moreover, some taxa include heteromorphic features, for example, 90% tricolpate and 10% dicolpate in *C. rumelica*, *Conringia orientalis*, and *L. latifolium*; 95% tricolpate and 5% monocolpate in *C. jonthlaspi*; and 90% tricolpate and 10% tetracolpate in *B. plantaginea*. Furthermore, the colpus dimension of the examined taxa has varied between 6.91 (*Sinapis arvensis*) and 23.98 (*Alyssum szowitsianum*) µm in length, and between 2.05 (*Alyssum murale* var. *murale*) and 4.95 (*Hesperis persica*) µm in width. The colpi have irregular and regular borders, acute ends, and granulate sheaths (Figures1–3 and Table 2).

The exine thickness has ranged from 1.08 (*Alyssum haussknechtii*) to 2.37 (*Iberis sempervirens*) µm, and it is mostly thicker in the apertural parts. The intine thickness is between 0.31 (*Aubrieta canescens* subsp. *canescens*) and 1.18 (*A. murale* var. *murale*) µm. The pollen surfaces in the studied taxa are reticulate (Lumina, 0.5–1 µm), micro reticulate (Lumina, <0.5 µm), coarse reticulate (Lumina,>1 µm), micro reticulate-foveolate, or coarse reticulate-foveolate with smooth or meandering muri. Lumina involves in 4 or 7 angular polygonal or irregular cells. The lumina diameter has varied between 0.18 (*A. haussknechtii*) and 2.18 (*Rapistrum rugosum*) µm.

A dendrogram has been created as a result of the cluster analysis of the examined taxa based on the variation of 12 characteristics in 44 taxa. The co-phenetic correlation coefficient is calculated to find the correlation between

the dendrogram and similarity matrix. The co-phenetic correlation between the coefficient matrix (similarity matrix) and tree matrix (dendrogram) has found to be 0.57.

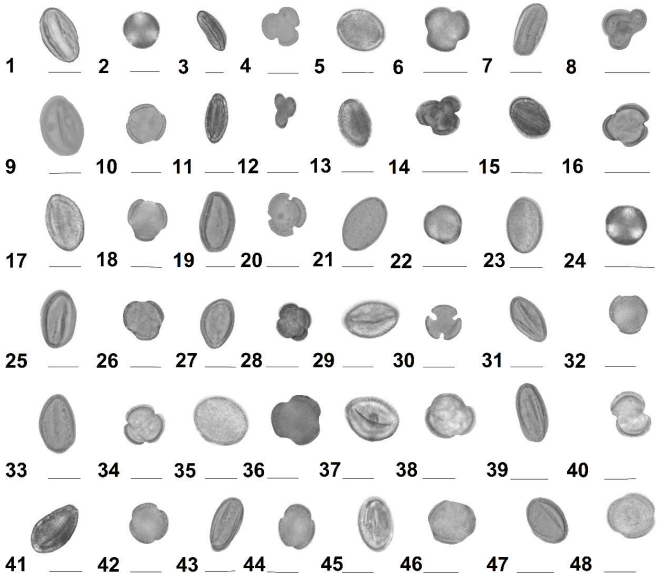

Figure 1. Light microscope pictures of the examined pollen; 1-2: *Alliaria petiolata*, 3-4: *Alyssoides utriculata* var. *utriculata*, 5-6: *Alyssum haussknechtii*, 7-8: *A. murale* var. *murale*, 9-10: *A. parviflorum*, 11-12: *A. sibiricum*, 13-14: *A. szowitsianum*, 15-16: *Arabis caucasica* subsp. *brevifolia*, 17-18: *A. caucasica* subsp. *caucasica*, 19-20: *A. sagittata*, 21-22: *Aubrieta canescens* subsp. *cilicica*, 23-24: *A. canescens* subsp. *canescens*, 25-26: *A. deltoidea*, 27-28: *Barbarea plantaginea*, 29-30: *B. vulgaris*, 31-32: *Berteroa mutabilis*, 33-34: *Bornmuellera kiyakii*, 35-36: *Cakile maritima*, 37-38: *Caleapina irregularis*, 39-40: *Camelina rumelica*, 41-42: *Cardamine bulbifera*, 43-44: *C. hirsuta*, 45-46: *C. impatiens* var. *pectinata*, 47-48: *C. lazica* (Scale bars: 10 µm, equatorial axis: odd numbers, polar axis: even numbers).

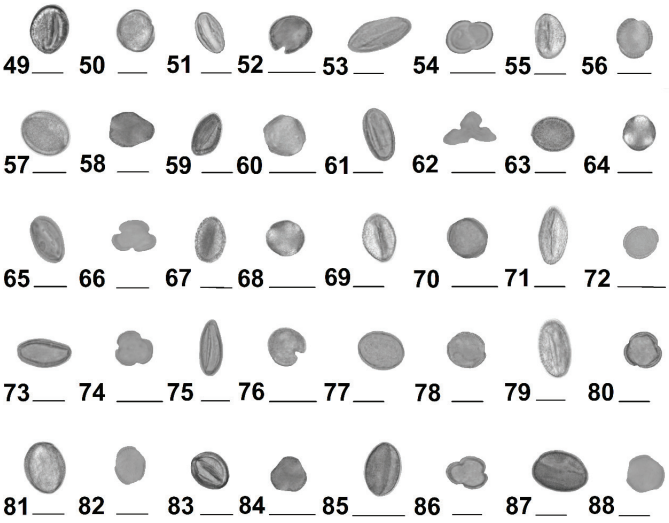

Figure 1. Light microscope pictures of the examined pollen; 49-50: *Cardamine uliginosa*, 51-52: *Clypeola jonthlaspi*, 53-54: *Conringia orientalis*, 55-56: *Draba bruniifolia* subsp. *olympica*, 57-58: *D. verna*, 59-60: *Erysimum crassipes*, 61-62: *E. cuspidatum*, 63-64: *Hesperis persica*, 65-66: *Iberis sempervirens*, 67-68: *I. spruneri*, 69-70: *Isatis arenaria*, 71-72: *I. glauca* subsp. glauca, 73-74: *Lepidium draba*, 75-76: *L. latifolium*, 77-78: *Matthiola montana*, 79-80: *Nasturtium officinale*, 81-82: *Rorippa amphibia*, 83-84: *Rapistrum rugosum*, 85-86: *Sinapis arvensis*, 87-88: *Turritis laxa* (Scale bars: 10 µm, equatorial axis: odd numbers, polar axis: even numbers).

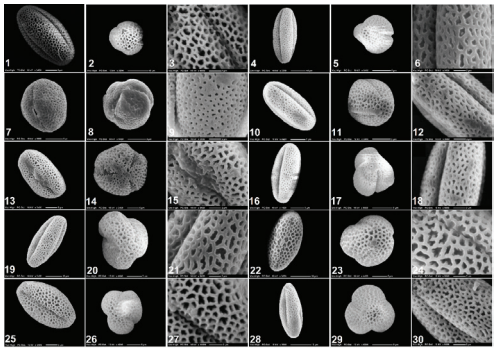

Figure 2. SEM pictures of the examined pollen; 1–3: *Alliaria petiolata*, 4–6: *Alyssoides utriculata* var. *utriculata*, 7–9: *Alyssum haussknechtii*, 10–12: *A. murale* var. *murale*, 13–15: *A. parviflorum*, 16–18: *A. sibiricum*, 19–21: *A. szowitsianum*, 22–24: *Arabis caucasica* subsp. *brevifolia*, 25–27: *A. caucasica* subsp. *caucasica*, 28–30: *A. sagittata*.

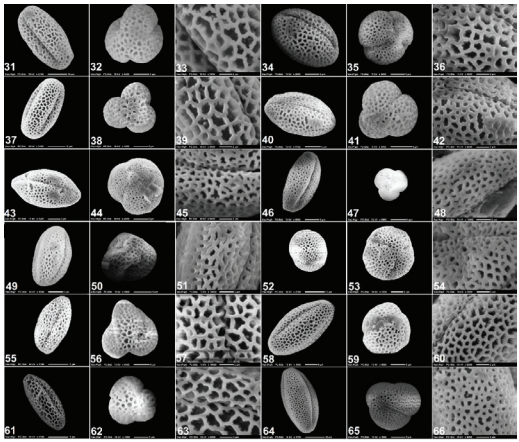

Figure 2. SEM pictures of the examined pollen; 31–33: *Aubrieta canescens* subsp. *cilicica*, 34–36: *A. canescens* subsp. *canescens*, 37–39: *A. deltoidea*, 40–42: *Barbarea plantaginea*, 43–45: *B. vulgaris*, 46–48: *Berteroa mutabilis*, 49–51: *Bornmuellera kiyakii*, 52–54: *Cakile maritima*, 55–57: *Caleapina irregularis*, 58–60: *Camelina rumelica*, 61–63: *Cardamine bulbifera*, 64–66: *C. hirsuta*.

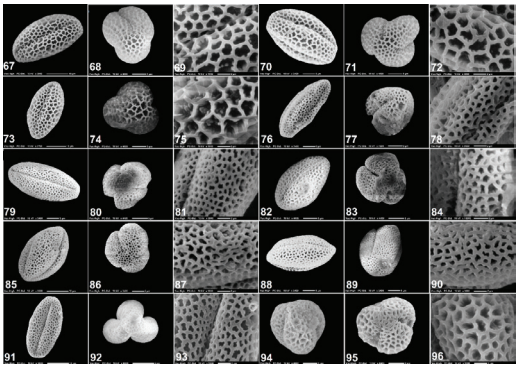

Figure 2. SEM pictures of the examined pollen; 67–69: *Cardamine impatiens* var. *pectinata*, 70–72: *C. lazica*, 73–75: *Cardamine uliginosa*, 76–78: *Clypeola jonthlaspi*, 79–81: *Conringia orientalis*, 82–84: *Draba bruniifolia* subsp. *olympica*, 85–87: *D. verna*, 88–90: *Erysimum crassipes*, 91–93: *E. cuspidatum*, 94–96: *Hesperis persica*.

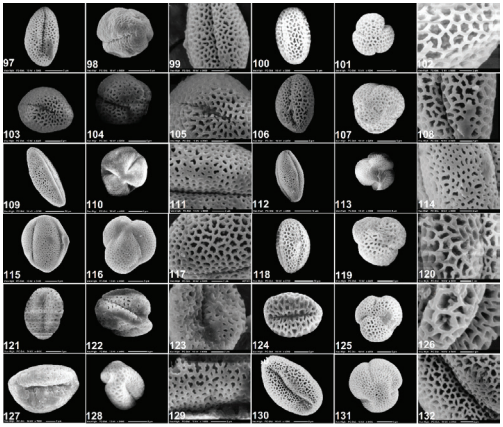

Figure 2. SEM pictures of the examined pollen; 97–99: *Iberis sempervirens*, 100–102: *I. spruneri*, 103–105: *Isatis arenaria*, 106–108: *I. glauca* subsp. glauca, 109–111: *Lepidium draba*, 112–114: *L. latifolium*, 115–117: *Matthiola montana*, 118–120: *Nasturtium officinale*, 121–123: *Rorippa amphibia*, 124–126: *Rapistrum rugosum*, 127–129: *Sinapis arvensis*, 130–132: *Turritis laxa*.

Table 2. *Pollen characters of the studied taxa: colpus length (Clg), colpus width (Clt), apocolpidium (Apo), outline of a pollen grain as viewed from a pole (Amb), standard deviation (±), see Table 1 for taxon abbreviations).*

Taxon	Pollen shape	P (µm) (1)	E (µm) (2)	(P/E) (3)	Colpus number	Aperture type	Ornamentation	Colpus size Clg (µm) (4)	Clt (µm) (5)	Clg/Clt (6)	Apo (µm) (7)	Amb (8)	Lumina (µm) (9)	Muri (µm) (10)	Intine (µm) (11)	Exine (µm) (12)
Alliaria petiolata	Prolate	18.25±017	12.31±0.38	1.48	3	Tricolpate	Reticulate	17.59±036	2.51±039	7.00	6.79±0.56	16.54±048	0.68±012	0.31±008	0.56±0.04	1.21±0.06
Alyssoides utriculata var. *utriculata*	Pergrolate	21.34±035	10.26±0.44	2.07	3	Tricolpate	Reticulate	20.41±028	2.92±018	6.98	3.51±033	11.97±036	0.71±018	0.46±004	0.64±0.06	1.59±0.08
Alyssum hamiltonschultzii	Subprolate	15.86±045	13.71±0.37	1.15	3	Tricolpate	Micro reticulate-Foveolate	12.18±037	4.09±015	2.97	2.09±044	7.73±0.27	0.18±008	0.53±012	0.49±0.12	1.08±0.12
Alyssum murale var. *murale*	Prolate	18.41±049	10.29±0.33	1.78	3	Tricolpate	Reticulate	14.74±051	2.05±045	7.19	4.16±021	14.58±041	0.52±012	0.28±015	1.18±0.08	1.25±0.15
Alyssum parviflorum	Prolate	15.33±027	10.63±0.30	1.44	3	Tricolpate	Reticulate	14.53±044	3.37±021	4.31	4.88±036	10.86±024	0.58±008	0.33±008	0.56±0.15	2.07±0.10
Alyssum sibiricum	Prolate	14.04±018	8.72±0.15	1.61	3	Tricolpate	Reticulate-Foveolate	18.62±056	2.96±044	6.29	4.02±053	8.41±0.33	0.56±010	0.41±012	0.45±0.12	1.33±0.12
Alyssum szovitsianum	Pergrolate	24.25±044	10.33±0.18	2.34	3	Tricolpate	Coarse reticulate	23.98±065	4.71±027	5.09	3.72±018	12.35±024	1.38±012	0.48±006	0.32±0.04	1.15±0.08
Arabis concaviscrosubsp. brevifolia	Prolate	20.46±027	12.61±0.21	1.62	3	Tricolpate	Coarse reticulate	19.87±033	4.09±048	4.85	6.35±024	15.97±063	1.62±018	0.56±012	0.40±0.06	1.29±0.08
Arabis caucasica subsp. *caucasica*	Prolate	23.41±048	13.29±0.28	1.76	3	Tricolpate	Coarse reticulate	17.79±054	3.54±036	5.02	4.07±015	15.44±036	1.69±024	0.37±009	0.56±0.08	1.32±0.12
Arabis sagittata	Pergrolate	21.05±036	9.13±0.24	2.30	3	Tricolpate	Reticulate	16.81±048	3.65±027	4.60	4.29±012	10.73±027	0.78±026	0.36±015	0.42±0.04	2.11±0.16
Aubrieta canescens subsp. *canescens*	Prolate	22.09±027	11.37±0.21	1.94	3	Tricolpate	Coarse reticulate	20.45±041	4.79±033	4.26	7.11±021	18.41±033	1.85±031	0.29±012	0.38±0.04	1.17±0.12
Aubrieta canescens subsp. *canescens*	Subprolate	17.34±021	13.86±0.19	1.25	3	Tricolpate	Coarse reticulate-Foveolate	15.92±045	4.15±021	3.83	3.87±015	13.62±045	1.23±036	0.41±018	0.31±0.04	1.23±0.14
Aubrieta deltoidea	Pergrolate	24.52±024	11.97±0.33	2.04	3	Tricolpate 90%	Coarse reticulate	21.08±033	4.82±027	4.37	9.25±033	19.85±027	1.88±041	0.45±009	0.42±0.06	1.19±0.08
Barbarea plantaginea	Prolate	17.44±049	12.51±0.38	1.39	3-4	Tricolpate, 10% Tetracolpate	Reticulate	16.45±036	3.71±036	4.43	5.42±021	14.06±024	0.91±029	0.51±012	0.37±0.08	1.86±0.10
Barbarea vulgaris	Prolate	23.56±045	14.74±0.51	1.59	3	Tricolpate	Reticulate	18.69±048	4.18±027	4.47	2.61±018	6.79±0.21	0.95±032	0.44±006	0.41±0.04	2.18±0.15
Berteroa mutabilis	Prolate	18.17±035	10.29±0.48	1.76	3	Tricolpate	Micro reticulate	15.41±035	3.05±015	5.05	3.83±039	11.32±036	0.41±008	0.51±008	0.44±0.06	2.03±0.08
Bornmuellera kiyakii	Subprolate	16.09±054	12.75±0.33	1.26	3	Tricolpate	Reticulate	14.90±027	2.62±033	5.68	2.94±024	9.81±0.33	0.56±012	0.62±014	0.56±0.04	1.79±0.12
Cakile maritima	Prolate-Spheroidal	20.11±027	17.93±0.36	1.12	3	Tricolpate	Reticulate	16.74±024	4.84±021	3.45	3.05±033	7.55±0.18	0.61±015	0.45±012	0.55±0.04	1.57±0.06
Calepina irregularis	Prolate	20.59±039	13.07±0.24	1.57	3	Tricolpate 90%	Coarse reticulate	18.56±033	4.91±065	3.78	2.66±012	15.70±027	1.29±036	0.44±021	0.43±0.06	1.42±0.10
Camelina rumelica	Pergrolate	22.42±044	11.08±0.33	2.02	2-3	Tricolpate, 10% Dicolpate	Coarse reticulate	15.51±044	4.88±039	3.17	1.49±024	13.79±036	1.18±041	0.51±015	0.45±0.04	1.48±0.12
Cardamine bulbifera	Pergrolate	21.54±037	10.73±0.44	2.01	3	Tricolpate	Coarse reticulate	19.36±047	3.73±015	5.19	5.26±033	11.48±033	2.02±036	0.49±016	0.41±0.04	2.14±0.15
Cardamine hirsuta	Pergrolate	24.79±024	9.88±0.36	2.50	3	Tricolpate	Micro reticulate	21.03±041	3.11±024	6.76	4.23±018	12.86±018	0.38±016	0.54±012	0.48±0.10	2.17±0.12

Continuation of Table 2 (*Colpus length (Clg), colpus width (Clt), apocolpidium (Apo), outline of a pollen grain from a polar view (Amb), standard deviation (±), see Table 1 for taxon abbreviations).*

Taxon	Pollen shape	P (um) (1)	E (E..um) (2)	(P/E) (3)	Colpus number	Aperture type	Ornamentation	Colpus size Clg (um) (4)	Colpus size Clt (um) (5)	Clg/Clt (6)	Apo (um) (7)	Amb (um) (8)	Lumina (um) (9)	Muri (um) (10)	Intine (um) (11)	Exine (um) (12)
Cardamine impatiens var. pectinata	Perprolate	22.48±021	11.01±0.18	2.04	3	Tricolpate	Coarse reticulate	19.57±024	2.77±0.18	7.06	6.17±027	15.09±041	1.92±029	0.33±008	0.52±0.04	1.79±008
Cardamine kitaica	Prolate	20.65±027	14.49±0.47	1.42	3	Tricolpate	Coarse reticulate	20.01±021	4.19±0.27	4.78	4.86±021	15.37±024	2.05±036	0.45±012	0.56±0.08	2.10±016
Cardamine uliginosa	Prolate	23.81±044	12.35±0.33	1.92	3	Tricolpate	Coarse reticulate	16.39±033	4.11±0.36	3.98	5.62±036	9.45±0.33	2.17±0.45	0.39±008	0.52±0.04	1.89±012
Clypeola jonthlaspi	Prolate	18.53±018	11.39±0.24	1.62	1-3	95% Tricolpate, 5% Monocolpate	Reticulate	14.86±061	2.79±0.33	5.32	4.43±027	12.86±027	0.62±021	0.37±015	0.43±0.06	1.97±016
Conringia orientalis	Perprolate	25.29±036	10.98±0.18	2.30	2-3	90% Tricolpate, 10% Dicolpate	Micro reticulate	17.15±054	4.85±021	3.53	6.25±024	11.12±015	0.41±018	0.44±010	0.47±0.08	1.81±011
Draba bruniifolia subsp. *olympica*	Prolate	17.77±039	10.81±0.33	1.64	3	Tricolpate	Reticulate	14.77±047	3.16±0.28	4.67	3.91±018	10.39±021	0.79±024	0.48±012	0.61±0.06	2.14±015
Draba cerviana	Prolate	20.26±027	14.85±0.21	1.36	3	Tricolpate	Coarse reticulate	19.85±033	2.81±0.18	7.06	5.14±021	8.64±0.24	1.14±027	0.35±008	0.45±0.04	1.72±018
Erysimum crassipes	Prolate	17.04±033	12.36±0.45	1.37	3	Tricolpate	Reticulate	14.81±027	2.43±0.21	6.09	6.56±033	9.77±0.36	0.83±021	0.42±015	0.38±0.04	1.33±008
Erysimum cuspidatum	Perprolate	23.48±0.51	10.52±0.69	2.23	3	Tricolpate	Reticulate	18.73±065	3.65±0.45	5.13	4.28±036	13.15±018	0.97±033	0.44±018	0.36±0.06	1.18±008
Hesperis pestrica	Subprolate	15.67±048	11.74±0.27	1.33	3	Tricolpate	Coarse reticulate	14.49±058	4.95±0.36	2.92	4.53±027	12.44±039	1.66±024	0.56±012	0.39±0.04	1.46±010
Iberis sempervirens	Perprolate	14.83±027	7.19±0.36	2.06	3	Tricolpate	Reticulate	12.46±033	3.51±0.41	3.54	3.97±018	8.51±0.12	0.51±018	0.39±004	0.68±0.12	2.37±021
Iberis spruneri	Prolate	15.40±053	10.17±0.39	1.51	3	Tricolpate	Coarse reticulate	16.68±045	3.96±0.39	4.21	5.04±021	15.23±015	1.84±0.10	0.48±008	0.51±0.08	2.01±012
**Isatis armena*	Subprolate	15.63±024	12.28±0.21	1.27	3	Tricolpate	Reticulate	9.92±0.18	2.77±012	3.58	3.71±044	13.86±024	0.83±015	0.43±010	0.49±0.04	2.08±010
Isatis glauca subsp. *glauca*	Perprolate	22.19±021	10.93±0.33	2.03	3	Tricolpate	Coarse reticulate	16.21±049	3.65±033	4.44	4.26±039	8.73±0.27	1.19±024	0.51±015	0.54±0.06	2.23±018
Lepidium draba	Prolate	17.26±045	11.34±0.27	1.52	3	Tricolpate	Micro reticulate-Foveolate	16.95±033	4.88±027	3.47	4.65±041	7.92±0.33	0.37±012	0.38±008	0.44±0.08	1.57±015
Lepidium latifolium	Perprolate	21.99±038	7.30±0.24	3.01	2-3	90% Tricolpate, 10% Dicolpate	Micro reticulate	21.38±036	4.34±0.45	4.92	4.53±027	10.77±024	0.42±021	0.45±006	0.45±0.10	1.66±012
Matthiola montana	Prolate-Spheroidal	12.76±033	11.94±0.45	1.06	3	Tricolpate	Reticulate	12.19±024	4.59±0.18	2.65	3.14±036	5.19±0.24	0.96±015	0.49±012	0.38±0.03	1.63±007
Nasturtium officinale	Perprolate	22.42±049	11.05±0.36	2.02	3	Tricolpate	Coarse reticulate	20.52±018	4.73±012	4.33	7.05±024	8.84±0.39	1.75±033	0.51±015	0.46±0.06	1.57±014
Rorippa amphibia	Prolate	20.77±018	11.09±0.28	1.87	3	Tricolpate	Micro reticulate	8.58±0.33	2.30±015	3.73	2.98±033	7.61±0.30	0.31±012	0.63±008	0.41±0.08	1.49±012
Rapistrum rugosum	Prolate-Spheroidal	12.45±036	11.23±0.45	1.10	3	Tricolpate	Coarse reticulate	11.73±027	3.99±0.24	2.93	2.71±018	8.56±0.33	2.18±041	0.69±010	0.55±0.12	1.76±010
Sinapis arvensis	Subprolate	10.19±024	8.38±0.27	1.21	3	Tricolpate	Micro reticulate	6.91±0.36	2.78±027	2.48	4.28±036	6.71±0.27	0.47±010	0.45±012	0.45±0.10	2.24±018
Turritis laxa	Prolate	21.84±069	16.05±0.51	1.36	3	Tricolpate	Reticulate	16.54±045	2.95±0.39	5.60	6.12±041	12.83±045	0.62±015	0.33±009	0.63±0.08	1.99±015

4. Discussion

Reviewing the morphological characters of the pollen was useful in the separation of the taxa. Some palynological studies have been carried out on the taxa of the family [Inceoglu and Karamustafa (1977) (32 taxa in family Brassicaceae), Perveen et al. (2004) (77 taxa in family Brassicaceae), Khan (2004) (8 taxa in genus *Arabidopsis*), Pınar et al. (2009) (25 taxa in genus *Hesperis*), Mutlu and Erik (2012) (22 taxa in genus *Arabis*), Kızılpınar et al. (2012) (5 taxa in genus *Malcolmia*), Sagun and Auer (2017) (13 taxa in tribe Camelineae), Kaya et al. (2017) (6 taxa in genus *Malcolmia*), Karaismailoğlu (2017) (12 taxa in genus *Aethionema*), Karaismailoğlu and Erol (2019) (22 taxa in genus *Thlaspi*)]. In addition to these palynological knowledge, this investigation included a statistical assessment of the pollen characters to create taxonomical correlations among the 44 taxa of family Brassicaceae from Turkey.

The most seen pollen shape in the studied taxa was prolate (21 taxa), followed by perprolate (14 taxa), subprolate (6 taxa), and prolate-spheroidal (3 taxa) (Figures 1–2 and Table 2). The number of seen pollen shapes was suitable with the results of Khalik et al. (2002), Mutlu and Erik (2012), Karaismailoğlu (2017), and Karaismailoğlu and Erol (2019), who examined the pollen of some other genera belonging to the family Brassicaceae, and faced with similar rankings.

Features of the aperture and exine structure have been characterized as an important principle in the explanation of the phylogenetic relations among the studied taxa in several studies (Cronquist, 1968; Takhtajan, 1980; Karaismailoğlu, 2017; Karaismailoğlu and Erol, 2019). The most seen aperture type was tricolpate, while *B. plantaginea*, *C. rumelica*, *C. jonthlaspi*, *C. orientalis*, and

L. latifolium include different forms (Table 2 and Figures 1–2). These variances in the aperture type were described as heteromorphy, which is leads to the emergence of polyploid lineages and supported by many as a strategy for long-lived versus short-lived pollen (Nadot et al., 2000), in pollen by Inceoglu and Karamustafa (1977) and Karaismailoğlu and Erol (2019).

The pollen exine surface structures have a significant role in discriminating some closely correlated taxa at the species and genus levels within the family Brassicaceae (Khalik et al., 2002; Karaismailoğlu and Erol, 2019). In this work, the pollen surface types were found to be reticulate, coarse reticulate, micro reticulate, microreticulate-foveolate, and coarse reticulate-foveolate (Table 2). Most of the studied taxa exhibited a reticulate (coarse or micro) exine surface structure; however, *Alyssum haussknechtii*, *Alyssum sibiricum*, *Aubrieta canescens* subsp. *canescens*, and *Lepidium draba* displayed both reticulate and foveolate surface structures. According to Anchev and Deneva (1997), and Karaismailoğlu and Erol (2019), the family Brassicaceae has two types of exine surface structures; reticulate and foveolate. This conjecture is consistent with the outcome of the present study.

According to Kovach (2007), the character variations have shown as a whisker plot in Figure 3. Accordingly, the sizes and colpus, apocolpidium, and shape and diameter of the amb, lumina, and exine thickness in the examined taxa displayed significant differences that may aid in determining the systematic relationships of the examined taxa, unlike the muri and intine thickness. The obtained outcomes from this study were parallel with those of previous studies including taxa from Turkey (Inceoglu and Karamustafa, 1977; Khan, 2004; **Pınar et al.**, 2009; Mutlu and Erik, 2012; Karaismailoğlu, 2017; Sagun and Auer, 2017; Karaismailoğlu and Erol, 2019).

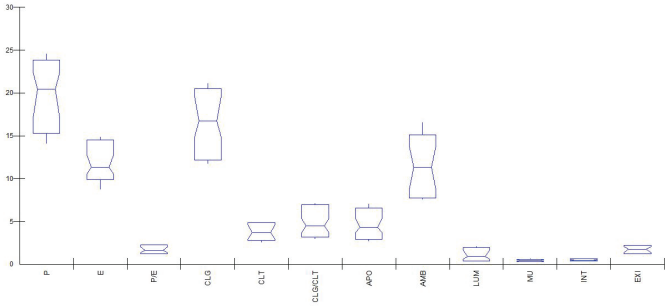

Figure 3. The variations of palynological characteristics for the examined taxa: outline of a pollen grain as viewed from a pole (Amb), apocolpidium (Apo), colpus length (Clg), colpus width (Clt), equatorial axis (E), polar axis (P).

The cluster analyses divided the taxa into 2 major clusters, A and B (B1: B11 and B12, B2: B21 and B22). Cluster A comprised *Sinapis arvensis* and *Isatis arenaria* (2 taxa). Cluster B11 comprised *Draba verna*, *Turritis laxa*, *Erysimum crassipes*, and *Bornmuellera kiyakii* (4 taxa). Cluster B12 included *Rorippa amphibia*, *Matthiola montana*, *Cakile maritima*, and *Alyssum haussknechtii* (4 taxa). Cluster B21 comprised *Nasturtium officinale*, *Lepidium draba*, *Barbarea vulgaris*, *Conringia orientalis*, *Isatis glauca* subsp. *glauca*, *Cardamine uliginosa*, *Arabis caucasica* subsp. *caucasica*, *Lepidium latifolium*, *Alyssum szowitsianum*, *Cardamine impatiens* var. *pectinata*, *C. bulbifera*, *C. hirsuta*, *Iberis sempervirens*, *Erysimum cuspidatum*, *Arabis sagittata*, and *Alyssoides utriculata* var. *utriculata* (16 taxa). Cluster B22 comprised 16 taxa (Figure 4). A separate clad in cluster B was formed for *Alyssum sibiricum*. In addition, *Rapistrum rugosum* formed a separate clad from clusters A and B and showed quite different cases from the other tested taxa. *Berteroa mutabilis* and *Draba bruniifolia* subsp. *olympica* were the

most closely related taxa; however, *Rapistrum rugosum* and *Aubrieta deltoidea* were the most distantly related taxa (Figures 4 and 5). Clusters B21 and B22 contained the highest number of taxa compared to the other clusters. This situation may be the reason why clusters B21 and B22 include taxa with primitive characters and taxa in other clusters. Also, the studied palynological characters are important features in discriminating of the examined taxa within *Cardamine* and *Aubrieta* genera. The cluster analysis outcome shows that the palynological features of the studied taxa had prominent variations and offer significant benefits to the systematics of the taxa within the family.

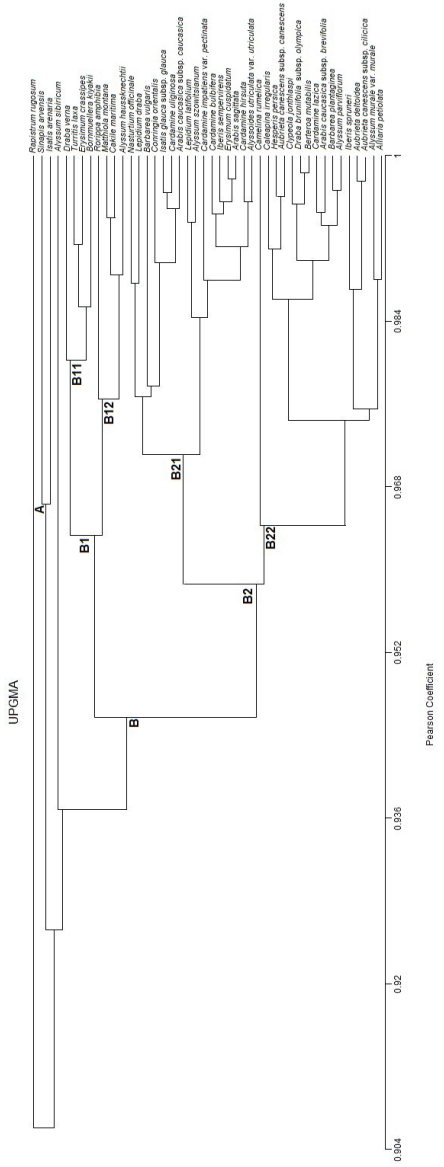

Figure 4. *UPGMA clustering of the studied taxa based on palynological characteristics.*

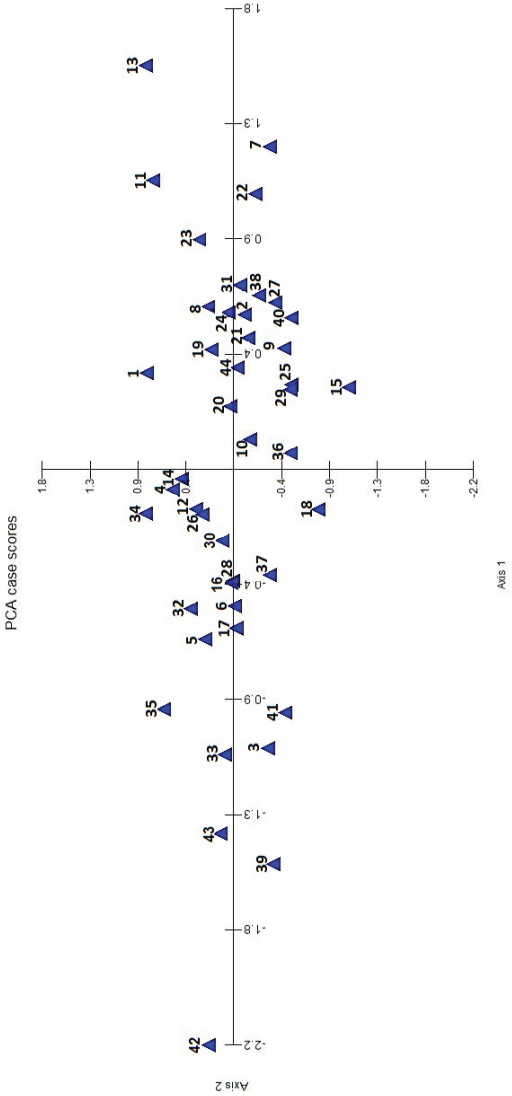

Figure 5. Principal component analysis (PCA) of the studied taxa based on palynological characteristics (see Table 1 for taxon abbreviations).

In conclusion, examining pollen of the studied taxa of Brassicaceae offers noteworthy contributions to the systematics of taxa within the family. These can be listed as follows:

1- A detailed pollen study was done for the first time, with the highest number of studied taxa in the family from Turkey.

2- The pollen features such as pollen and colpus sizes, surface ornamentation types, outline of a pollen grain from a polar view (Amb) diameter, apocolpidium, intine and exine thicknesses of the examined taxa exhibited prominent variations and thus provided important contributions to the systematics of the taxa within the family. These prominent features allowed easier identification of morphologically similar taxa such as *Aubrieta deltoidea-Aubrieta canescens* subsp. *canescens*, *Alyssum parviflorum-Alyssum sibiricum*, *Arabis caucasica* subsp. *caucasica-Arabis caucasica* subsp. *brevifolia*, *Erysimum crassipes-Erysimum cuspidatum* and *Lepidium draba-Lepidium latifolium*.

3- The outcomes were assessed with statistical analysis and their reliability was defined.

4- A key was provided for the identification of the studied taxa based on pollen characters.

Key to studied taxa, based on pollen characters

1.Pollen shapes are prolate or prolate-spheroidal 2

2.Pollen shapes are prolate.....3

3.Pollen are of heteromorphic features.....4

4.Clg/Clt >5..... *Clypeola jonthlaspi*

4.Clg/Clt <5..... *Barbarea plantaginea*

3.Pollen are of homomorphic features.....5

5.Pollen ornamentation type is reticulate or reticulate-foveol ate.....6

6.Reticulate-foveolate.....*Alyssum sibiricum*

6.Reticulate.....7

7.Clg/Clt >5.....8

8.Apocolpidium <5 µm.....9

9.Exine thickness <1.5 µm.... *Alyssum murale* var. *murale*

9.Exine thickness >1.5 µm.....*Alyssum parviflorum*

8.Apocolpidium >5 µm.....10

10.Amb >15 µm.....*Alliaria petiolata*

10.Amb <15 µm..... ..*Erysimum crassipes*

7.Clg/Clt<5.....11

11.Apocolpidium >5 µm.....*Turritis laxa*

11.Apocolpidium <5 µm.....12

12.Intine thickness <0.5 µm.....*Barbarea vulgaris*

12.Intine thickness >0.5 µm..... *Draba bruniifolia* subsp. *olympica*

5.Pollen ornamentation type is microreticulate, microreticulate-foveolate or coarse reticulate.....13

13.Microreticulate-foveolate or microreticulate.....14

14.Microreticulate-foveolate..... *Lepidium draba*

14.Microreticulate.....15

15.Clg/Clt <5..... *Rorippa amphibia*

15.Clg/Clt >5..... *Berteroa mutabilis*

13.Coarse reticulate.....16

16.Clg/Clt >5.....17

17.Amb >15 µm..... *Arabis caucasica* subsp. *caucasica*

17.Amb <15 µm.....*Draba verna*

16.Clg/Clt <5.....18

18.Amb <15 µm.....*Cardamine uliginosa*

18.Amb >15 µm.....19

19.Lumina.>2 µm.....*Cardamine lazica*

19.Lumina <2 µm.....20

20.Intine thickness >0.5 µm..... *Iberis spruneri*

20.Intine thickness <0.5 µm.....21

21.Apocolpidium <5 µm.....*Caleapina irregularis*

21.Apocolpidium >5 µm.....22

22.Muri thickness >0.5 µm..... *Arabis caucasica* subsp. *brevifolia*

22.Muri thickness <0.5 µm..... *Aubrieta canescens* subsp. *cilicica*

2.Pollen shapes are prolate-spheroidal.....23

23.Pollen ornamentation type is coarse reticulate .... *Rapistrum rugosum*

23.Pollen ornamentation type is reticulate.....24

24.Intine thickness >0.5 µm.....*Cakile maritima*

24.Intine thickness <0.5 µm..... *Matthiola montana*

1.Pollen shapes are subprolate or perprolate.....25

25.Perprolate.....26

26.Pollen are of heteromorphic features 27

27.Pollen ornamentation type is coarse reticulate .... *Camelina rumelica*

27.Pollen ornamentation type is microreticulate 28

28.Apocolpidium >5 µm..... *Conringia orientalis*

28.Apocolpidium <5 µm..... *Lepidium latifolium*

26.Pollen are of homomorphic features.....29

29.Microreticulate..... *Cardamine hirsuta*

29.Coarse reticulate or reticulate.....30

30.Coarse reticulate.....31

31.Clg/Clt >5.....32

32.Apocolpidium <5 µm..... *Alyssum szowitsianum*

32.Apocolpidium >5 µm.....33

33.Intine thickness >0.5 µm..... *Cardamine impatiens* var. *pectinata*

33.Intine thickness <0.5 µm..... *Cardamine bulbifera*

31.Clg/Clt <5.....34

34.Apocolpidium <5 µm..... *Isatis glauca* subsp. *glauca*

34.Apocolpidium >5 µm.....35

35. Amb >15 µm..... *Aubrieta deltoidea*

35. Amb <15 µm..... *Nasturtium officinale*

30.Reticulate.....36

36.Clg/Clt >5.....37

37.Intine thickness >0.5 µm..... *Alyssoides utriculata* var. *utriculata*

37.Intine thickness <0.5 µm... *Erysimum cuspidatum*

36.Clg/Clt <5.....38

38.Intine thickness >0.5 µm..... *Iberis sempervirens*

38.Intine thickness <0.5 µm..... *Arabis sagittate*

25.Subprolate.....39

39.Reticulate, coarse reticulate, coarse reticulate-foveolate.....40

40.Reticulate.....41

41.Clg/Clt >5..... *Bornmuellera kiyakii*

41.Clg/Clt <5..... *Rorippa amphibia*

40.Coarse reticulate, coarse reticulate-foveolate....42

42.Coarse reticulate..... *Hesperis persica*

42.Coarse reticulate-foveolate..... .....*Aubrieta canescens* subsp. *canescens*

39.Microreticulate, microreticulate-foveolate.....43

43.Microreticulate.....*Sinapis arvensis*

43.Microreticulate-foveolate..... *Alyssum haussknechtii*

Acknowledgements

The author wishes to thank the professors at the İstanbul University, Division of Botany, for providing the facilities with some of the equipment.

REFERENCES

Al-Shehbaz, I.A., Beilstein, M.A. and Kellogg, E.A. (2006). Systematics and phylogeny of the Brassicaceae (Cruciferae): an overview. *Plant Systematics and Evolution, 259*, 89-120.

Al-Shehbaz, I.A., Mutlu, B. and Donmez, A.A. (2007). The Brassicaceae (Cruciferae) of Turkey, Updated. *Turkish Journal of Botany, 31,* 327-336.

Anchev, M. and Deneva, B. (1997). Pollen morphology of seventeen species from family Brassicaceae (Cruciferae). *Phytologica Balcanica, 3,* 75-82.

Brochmann, C. (1992). Pollen and seed morphology of Nordic *Draba* (Brassicaceae): phylogenetic and ecological implications. *Nordic Journal of Botany, 1,* 657-673.

Candan, F. and Öztürk Calı, I. (2015). Pollen micromorphology of four taxa of *Anemone coronaria* L. from Western Turkey. *Bangladesh Journal of Botany, 44,* 31-36.

Dogan, C. and Inceoglu, O. (1990). Pollen morphology of some *Isatis* L. taxa in Turkey. *Turkish Journal of Botany, 14,* 12-31.

Faegri, K. and Iversen, J. (1989). *Textbook of pollen analysis*. Chichester: Willey.

Filiz, E., Osma, E., Kandemir, A., Tombuloglu, H., Tombuloglu, G., Birbilener, S. and Aydın, M. (2014). Assessment of genetic diversity and phylogenetic relationships of endangered endemic plant *Barbarea integrifolia* DC. (Brassicaceae) in Turkey. *Turkish Journal of Botany, 38,* 1169-1181.

Franzke, A., Lysak, M.A., Al-Shehbaz, I.A., Koch, M.A. and Mummenhoff, K. (2011). Cabbage family affairs: The evolutionary history of Brassicaceae. *Trends Plant Science, 16, 108*-116.

Inceoglu, O. and Karamustafa, F. (1977). The pollen morphology of plants in Ankara region II. Cruciferae. *Com Fac Sci Ankara Ser C2, 21,* 111-118.

Karaismailoğlu, M.C. (2015). Morphological and anatomical features of seeds of Turkish *Romulea* taxa (Iridaceae) and their taxonomic significance. *Acta Botanica Croatica, 74,* 31-41.

Karaismailoğlu, M.C. (2017). Palynological features of eleven *Aethionema* taxa from Turkey and their systematic implications. *Bangladesh Journal of Plant Taxonomy, 24,* 197-204.

Karaismailoğlu, M.C. and Erol, O. (2018). Seed structure and its taxonomic implications for genus *Thlaspi* sensu lato sections *Nomisma*, *Thlaspi*, and *Pterotropis* (Brassicaceae). *Turkish Journal of Botany, 42,* 591-609.

Karaismailoğlu, M.C. and Erol, O. (2019). Pollen morphology of some taxa of *Thlaspi* L. sensu lato (Brassicaceae) from Turkey, and its taxonomical importance. *Palynology, 42,* 244-254.

Khalik, K.A., Maesen, L.J.G., Kopman, W.J.M. and Berg, R.G. (2002). Numerical taxonomic study of some tribes of Brassicaceae from Egypt. *Plant Systematics and Evolution, 233,* 207-221.

Khan, R. (2004). Studies on the pollen morphology of the genus *Arabidopsis* (Brassicaceae) from Pakistan. *Pakistan Journal of Botany, 36,* 229-234.

Kaya, A., Unal, M., Ozgokce, F., Dogan, B. and Martin, E. (2017). Pollen morphology of six species previously placed in *Malcolmia* (Brassicaceae) in Turkey. *Bangladesh Journal of Botany, 46,* 623-629.

Kızılpınar, I., Altınözlü, H. and Dogan, C. (2012). Pollen morphology of the some species of the genus *Malcolmia* (Brassicaceae). *Mellifera, 12,* 24-29.

Kiefer, M., Schmickl, R., German, D.A., Mandáková, T., Lysák, M.A., Al-Shehbaz, I.A., Franzke, A., Mummenhoff, K., Stamatakis, A. and Koch, M.A. (2014). BrassiBase: Introduction to a novel knowledge database on Brassicaceae evolution. *Plant Cell Physiol, 55,* 1-9.

Kovach, W.L. (2007). *MVSP - A Multi Variate Statistical Package for Windows, Ver. 3.1.* Pentraeth: Kovach Computing Services.

Mohammadi, S.A. and Prasanna, B.M. (2003). Analysis of genetic diversity in crop plants: Salient statistical tools and considerations. *Crop Science, 43,* 1235-1248.

Mutlu, B. and Erik, S. (2012). Pollen morphology and its taxonomic significance of the genus *Arabis* (Brassicaceae) in Turkey. *Plant Systematics and Evolution, 298,* 1931-1946.

Perveen, A., Qaiser, M. and Khan, R. (2004). Pollen flora of Pakistan-XLII. Brassicaceae. *Pakistan Journal of Botany, 36,* 683-700.

Pınar, N.M., Duran, A., Ceter, T. and Tuğ, G.N. (2009). Pollen and Seed Morphology of the Genus *Hesperis* L. (Brassicaceae) in Turkey. *Turkish Journal of Botany, 33,* 83-96.

Punt, W., Blackmore, S., Nilsson, S. and Le Thomas, A. (1994). *Glossary of pollen and spore terminology.* Utrect: Lab Palaeobot Palynol.

Sagun, V.G. and Auer, C. (2017). Pollen morphology of selected Camelineae (Brassicaceae). *Palynology, 41,* 255-266.

Wodehouse, R.P. (1935). *Pollen Grains.* New York: McGraw Hill.

DISTRIBUTION AND ECOLOGY OF MYXOMYCETES

Mustafa SEVİNDİK[1], Celal BAL[2], Demet YILMAZKAYA[3], Hasan AKGÜL[4], C. Cem ERGÜL[5]

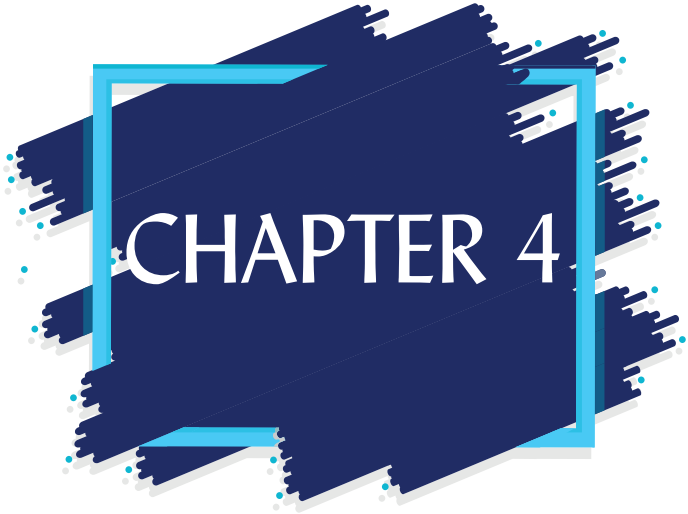

1 Department of Food Processing, Bahçe Vocational School, Osmaniye Korkut Ata University, Osmaniye, Turkey
2 Gaziantep University, Oguzeli Vocational School, Gaziantep, Turkey.
3 Gaziantep University, Science and Arts Faculty, Department of Biology, Gaziantep, Turkey.
4 Akdeniz University, Science Faculty, Department of Biology, Antalya, Turkey.
5 Bursa Uludağ University, Science Faculty, Department of Biology, Bursa, Turkey.

DISTRIBUTION AND ECOLOGY OF MYXOMYCETES

Mustafa SEVİNDİK[1], Celal BAL[2], Demet YILMAZKAYA[3], Hasan AKGÜL[4], C. Cem ERGÜL[5]

INTRODUCTION

Myxomycetes (plasmodial slime molds) are phagotrophic amoeboid eukaryotes that occur in association with decaying plant material in almost all types of terrestrial ecosystems. They are particularly abundant in forested regions where decaying logs, stumps, and dead leaves provide a plentiful supply of potential substrates. They inhabit all terrestrial ecosystems, feeding on bacteria and other microorganisms, in and on plant parts and plant remains (Eliasson, 2013; Baba, 2015a, Baba et al., 2018). Myxomycetes live predatory on other microorganisms such as bacteria, yeasts, algae, or true fungi, feed phagotrophically on bacteria, yeasts, spores of filamentous fungi, algae, and other protists the production of fruiting bodies and dispersal by spores, cause myxomycetes to appear similar to fungi (Baba, 2012a). They inhabit microenvironments in forest ecosystems, such as the bark surface of living trees, forest floor litter, and fallen trees decaying wood, forest floor litter, or the dung of herbivorous animals (Stephenson, 1989). The majority of

1 Department of Food Processing, Bahçe Vocational School, Osmaniye Korkut Ata University, Osmaniye, Turkey
2 Gaziantep University, Oguzeli Vocational School, Gaziantep, Turkey.
3 Gaziantep University, Science and Arts Faculty, Department of Biology, Gaziantep, Turkey.
4 Akdeniz University, Science Faculty, Department of Biology, Antalya, Turkey.
5 Bursa Uludağ University, Science Faculty, Department of Biology, Bursa, Turkey.

species are cosmopolitan, but a few species appear to be confined to the tropics or subtropics and some others have been collected only in temperate regions (Farr, 1976).

Myxomycetes are terrestrial organisms, but some species have been reported from aquatic habitats. Didymium aquatile, *Didymium difforme Physarum gyrosum, Physarum album* and *Fuligo cinerea* has been reported to complete its entire life cycle underwater and producing fruiting bodies (Rollins and Stephenson, 2011).

Temperature, moisture, pH, and the availability of decomposing plant material are principal factors occurrence of myxomycetes in nature (Stephenson and Stempen, 1994). The pH of the substrates potentially available to myxomycetes in a particular habitat also represents an important factor the distribution of these organisms. Although many myxomycetes appear to have a relatively wide pH tolerance, this is not the case for all species. Some species seemed to prefer an acidic substrate, whereas others never developed under low pH conditions. In general, members of the *Stemonitales* developed under more acidic conditions than did members of the *Physarales* and the *Trichiales* (Stephenson, 1989).

Life Cycle

The myxomycete life cycle involves two trophic stages, one consisting of uninucleate amoebae, with or without flagella, and the other consisting of a distinctive multinucleate structure, the plasmodium (Martin et al., 1983). Their life cycle includes myxamoebae, swarm cells, multinucleate plasmodia, microcysts, sclerotia and fruit bodies (Baba and Tamer, 2007). The life cycle starts with haploid, unicellular myxoflagellates and myxamoebae hatching from spores. The myxamoebae and plasmodia feed on bacteria, yeasts and other microorganisms associated

with soil, plant litter and other decomposing plant debris (Martin and Alexopoulos, 1969). The usual situation is for a single myxoamoeba to emerge from a spore, but a spore can yield up to four myxoamoebae. In the presence of adequate water, a myxamoeba may develop flagella. If environmental conditions turn unfavorable, the myxamoebae can form resistant structures referred to as microcysts. These myxamoebae are able to emerge when conditions improve. Eventually, two compatible myxamoebae from different populations can function as gametes and fuse to produce a diploid zygote. The zygote feeds, carries out synchronous nuclear divisions, and grows, ultimately producing a coenocytic trophic structure called a plasmodium. Under favorable conditions, the plasmodium gives rise to one or more fruiting bodies containing spores. The plasmodium is essentially a single cell that crawls around in its microhabitat, ingesting a wide array of different organisms, including algae, fungal spores, fungal hyphae, and even other protists. The plasmodium can form a resistant stage called a sclerotium if conditions become unfavorable. As is the case for microcysts, when suitable conditions return, the plasmodium can emerge and resume its activity (Figure 1).

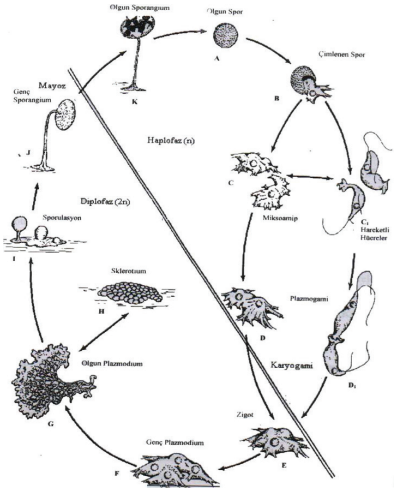

Figure 1. *Life cycle of a Heterothallic Myxomycetes*

Fruiting bodies form one of four general types: sporangium, plasmodiocarp, pseudoaethalium, or aethalium. The sporangium is a generally globose structure, usually less than 1 mm in diameter and is either stalked or sessile (Figure 2).

Figure 2. *Sporangium of Badhamia utricularis (Bull.) Berk. (Baba et al., 2013)*

The plasmodiocarp is a single mass of spores in a reticulate network that derives its shape from the plasmodial veins that mature in situ, and in some cases plasmodiocarp and sessile sporangia are produced by the same plasmodium(Figure 3).

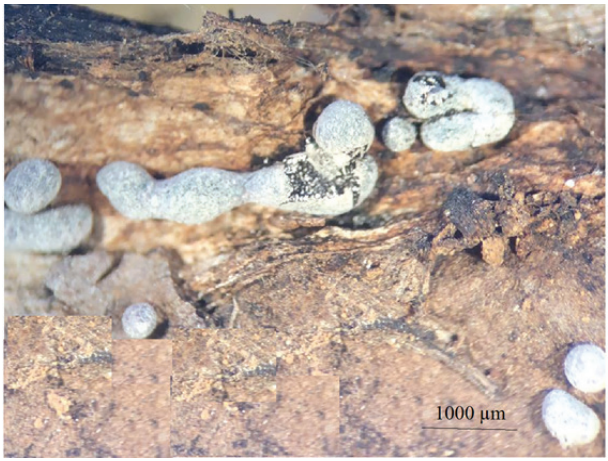

Figure 3. *Plasmodiocarp of Physarum bitectum G. Lister (Baba, 2015b)*

The aethalium is a single, sessile mass of spores that is often large and pulvinate, cushion- or mound-shaped, and the spores are sometimes supported by the pseudocapillitium, thread-like structures analogous to the capillitium. The spores are covered by the cortex, a thickened peridium. for example the genus *Lycogala*. (Figure 4).

Figure 4. *Aethalium of Lycogala epidendrum (L.) Fr. (Baba and*

Arslan, 2017b)

The pseudoaethalium is a fused mass of sporangia that outwardly looks like an aethalium. The surface is superficially divided by individual sporangial caps that, for example, have thread-like strands hanging from the corners of the caps, as in *Dictydiaethalium plumbeum* (Schumach.) Rostaf. (Figure 5).

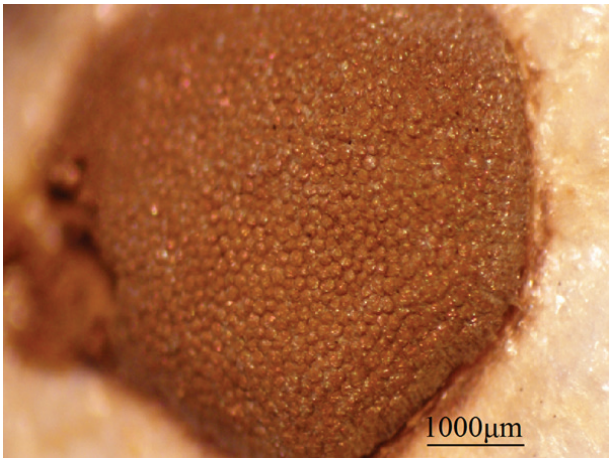

Figure 5. *Pseudoaethalium of Dictydiaethalium plumbeum (Schumach.) Rostaf. (Baba et al., 2008)*

Taxonomic orders

Myxomycetes consists of 1017 species worldwide (Lado, 2019). They have been known for more than 350 years based on Pankow's description of *Lycogala epidendrum* (L.) Fr. in 1654. There are six orders currently recognized in the Myxomycetes: *Echinosteliales*, *Liceales, Trichiales, Physarales,* and *Stemonitales*. The Ceratiomyxales is an order recognized in older texts, but is now placed in the Class Protostelia due to the presence of an externallyborne spore (Spiegel et al., 2004). Each spore located on an individual stalk. The Ceratiomyxales is the smallest order (4 species). The *Echinosteliales* is a small

order (20 species) characterized by a protoplasmodium, single, tiny sporangiate fruiting body, usually less than 1 mm. The *Liceales* (159 species) is fruiting bodies that lack a columella, true capillitium, and calcium carbonate. The *Trichiales* (191 species) are characterized by a trichiaceous plasmodium and fruiting bodies with light coloured spores in mass, the presence of a true capillitium, and absence of a columella and calcium carbonate. The Physarales is by far the largest order (421 species) and has large phaneroplasmodia and fruiting bodies with dark coloured spores in mass. Fruiting bodies have a true capillitium and granular or crystalline calcium carbonate. The *Stemonitales* (221 species) are characterized by an aphanoplasmodium and sporangia that may appear separate or pseudoaethalioid due to close grouping. The sporangia contain dark coloured spores in mass and are characterized by presence of a true capillitium and absence of calcium carbonate (Keller and Braun, 1999; Lado and Eliasson, 2017).

Distribution and Ecology

There are four major ecological groups of myxomycetes exist. These are the lignicolous, corticolous, litter-inhabiting, and coprophilous myxomycetes (Schnittler and Stephenson, 2000).

The lignicolous species inhabit dead and decaying wood abundant and widespread group. These species characteristically produce robust fruitings that can easily be observed in the field. Many of the more common and widely known myxomycete taxa, including various species of *Arcyria, Lycogala, Stemonitis* and *Trichia,* are predominantly lignicolous (Rojas et al., 2014). More commonly encountered species is *Perichaena depressa* which also occurs on twigs, ground litter and the bark surface of living trees. Among the species most likely to

be associated with coarse woody debris in tropical forests are *Arcyria denudata, Cribraria cancellata, Hemitrichia calyculata, Lycogala epidendrum, Physarella oblonga, Physarum stellatum* and *Stemonitis fusca. Ceratiomyxa fruticulosa*, a species usually confined to coarse woody debris (Rojas et al., 2014). (Figure 6).

Figure 6. *Lignicolous species; Perichaena depressa Lib. and Arcyria denudata (L.) Wettst. (Baba et al., 2016; Baba and Doğan, 2018)*

Corticolous species are associated with the bark surface of living or dead trees and plants. More than 100 species of "corticolous" myxomycetes have been reported from the bark. Some species of myxomycetes members of the genus are almost found on the bark, *Badhamia, Echinostelium, Licea*, and *Macbrideola* (Figure 7). Several factors influence the occurrence of these species in the bark microhabitat, including the surface texture of

the bark, the epiphytic load, water holding capacity, and pH (Mitchell, 1980).

Figure 7. *Corticolous species; Badhamia dubia and Echinostelium minutum (Baba et al., 2013)*

Litter-inhabiting species are associated with the complex mixture of plant parts that have fallen to the ground. This mixture consists largely of dead leaves, but also contains small twigs, pieces of bark, fruits, and flower parts. Long stalked members of the genus *Didymium*, *Physarales*, including *Didymium iridis*, tend to be exceedingly common on aerial litter. Three other species likely to be encountered in this microhabitat are *Lamproderma scintillans, Physarum compressum* and *P. melleum* (Rojas et al., 2014) (Figure 8).

Figure 8. *Litter-inhabiting species; Lamproderma scintillans and Physarum compressum (Baba et al., 2013)*

Coprophilous species occur on the dung of herbivores, approximately 100 species have been recorded from dung. Dung is a highly complex substrate, and the exact role of myxomycetes in the communities of organisms associated with its decomposition is not yet known (Eliasson and Lundqvist, 1979). One species (*Kelleromyxa fimicola*) appears to be adapted to passage through the digestive tract of herbivores. *Didymium trachysporum* is a coprophilous species (Figure 9).

Figure 9. *Coprophilous species; Didymium trachysporum (Baba et al., 2014)*

In addition to the four major ecological groups mentioned above, there are several other relatively minor ecological assemblages of myxomycetes. These include the soil-inhabiting, aerial litter inhabiting, foliocolous twig-inhabiting, bryophilous, and nivicolous myxomycetes.

Bryophilous species (*Barbeyella minutissima* and *Lepidoderma tigrinum*) are associated with bryophytes and the algal layers that occur along with bryophytes on decorticated wood in some microhabitats (Rollins and Stephenson, 2011).

Nivicolous species are associated with the edges of melting snowbanks across mountainous regions of the world. Members of this group have been reported from various ecological vegetation formations induced by elevational gradients; however, most species tend to be associated with the forested areas of mountains whereas only a couple species seem to be associated with true alpine vegetation, for example *Prototrichia metallica*, *Hemitrichia montana* (Figure 10) (Ronikier and Ronikier, 2009; Baba, 2018).

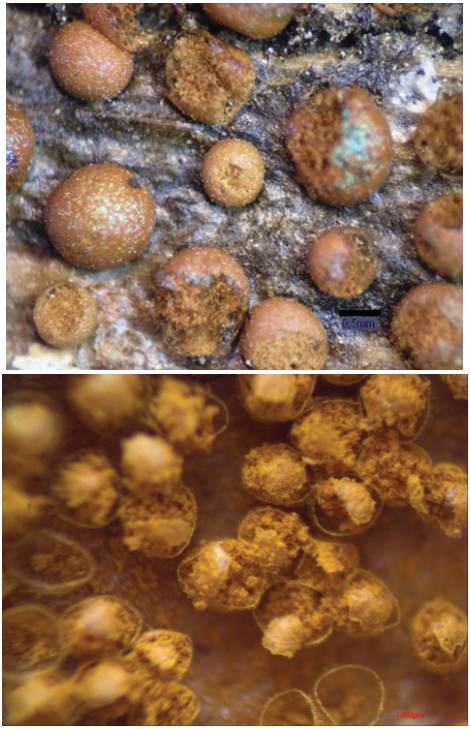

Figure 10. *Nivicolous species; Prototrichia metallica and Hemitrichia montana (Baba, 2008; Baba et al., 2016)*

Myxomycetes also are known to occur in forest soils (Kalyanasundaram, 1997; Stephenson et al., 2011). Various species of *Didymium* appear to be the most widespread

and abundant myxomycetes present in soil. Interestingly, myxomycetes seem to be relatively more abundant in grassland and agricultural soils than in forest soils (Figure 11) (Feest and Madelin, 1985; Madelin 1990).

Figure 11. *Myxomycetes in soil; Physarum cinereum and Didymium difforme (Baba, 2017)*

Arcyria cinerea, Didymium difforme and *D. squamulosum* tend to be associated with a wide range of different substrates and cosmopolit species all over the world (Figure 12).

Figure 12. *Cosmopolit species; Arcyria cinerea and Didymium squamulosum (Baba, 2012b)*

CONCLUSION

Microhabitats were more important than geographical locations or country in affecting myxomycete species distributions (Schnittler and Stephenson, 2000). Myxomycetes appear to be particularly abundant in temperate forests, but at least some species apparently occur in any terrestrial ecosystem with plants and plant detritus (Stephenson and Stempen, 1994). For example, they have been reported from deserts (Blackwell and Gilbertson, 1980) and high-latitude tundra (Stephenson and Laursen, 1993), where harsh environmental conditions place severe constraints on living organisms.

REFERENCES

A. Feest, M.F. Madelin, ‘‘A method for the enumeration of myxomycetes in soils and its application to a wide range of soils,’’ *FEMS Microbiology Ecology,* 31:103-109, 1985.

A. Ronikier, M. Ronikier, ‘‘How ‘alpine’ are nivicolous myxomycetes? A worldwide assessment of altitudinal distribution,’’ *Mycologia*, 101(1):1–16, 2009.

A.W. Rollins, S.L. Stephenson, ‘‘Global distribution and ecology of myxomycetes,’’ *Plant Biology*, 12(1): 1-14, 2011.

C. Lado, ‘‘An on line nomenclatural information system of Eumycetozoa,’’ Real Jardín Botánico, CSIC. Madrid, Spain. http://www.nomen.eumycetozoa.com. Last updated April 29, 2019.

C. Lado, U. Eliasson, ‘‘Taxonomy and Systematics: Current Knowledge and Approaches on the Taxonomic Treatment of Myxomycetes,’’ Chapter 7 p. 205-251. Myxomycetes: Biology, Systematics, Biogeography, and Ecology, 2017. http://dx.doi.org/10.1016/B978-0-12-805089-7.00007-X Elsevier

C. Rojas, R.G. Doss, ‘‘Does habitat loss affect tropical myxomycetes,’’ *Mycosphere*, 5: 692–700, 2014.

D.W. Mitchell, ‘‘A key to the corticolous myxomycetes,’’ The British Mycological Society, Cambridge, England, 1980.

F.W. Spiegel, S.L. Stephenson, H.W. Keller, D.L. Moore, J.C. Cavender, ‘‘Mycetozoans. In: G.M. Mueller, G.F. Bills and M.S. Foster, Editors, Biodiversity of Fungi,’’ Inventory and Monitoring Methods, Elsevier Academic Press, Amsterdam pp. 547–576, 2004.

G.W. Martin, C.L. Alexopoulos, ‘‘The Myxomycetes,’’ Iowa City: University of Iowa Press. 560, 1969.

G.W. Martin, C.L. Alexopoulos, M.L. Farr, ‘‘The Genera of Myxomycetes,’’ University of Iowa Press, Iowa City, USA, 1983.

H. Baba, ‘‘A New Myxomycetes Genus and three species record for Turkey,’’ *International Journal of Botany*, 4: 336-339, 2008.

H. Baba, ‘‘Diversity and Ecology of Myxomycetes in Antakya-Hatay (Turkey),’’ *The Journal of Fungus*, 3(1-2):5–11, 2012a.

H. Baba, ‘‘Investigation of Myxomycetes diversity on Kuseyr Mountain; Three new records in Hatay/Turkey,’’ *Fresen. Environ. Bull.*, 24(11): 4077-4086, 2015a.

H. Baba, ‘‘Miksomisetlerin alternatif üretim yöntemleri üzerine bir çalışma,’’ *The Herb Journal of Systematic Botany*, 25(1): 137-148, 2018.

H. Baba, ‘‘Myxomycetes of Mustafa Kemal University Campus and environs (Turkey),’’ *Turkish Journal of Botany*, 36: 769–777, 2012b.

H. Baba, ‘‘Some Mycetozoa (Myxomycetes) members from zorkun high plateau (Osmaniye),’’ *Anatolian Journal of Botany*, 1(2):37−40, 2017.

H. Baba, ‘‘The genus *Physarum* (Myxomycetes) checklist in Turkey,’’ *Biological Diversity and Conservation*, 8(3): 20-24, 2015b.

H. Baba, A.Ü. Tamer, ‘‘A study on the Myxomycetes in Manisa,’’ *The Herb Journal of Systematic Botany*, 14(2): 179–196, 2007.

H. Baba, A.Ü. Tamer, F. Kalyoncu, ‘‘New Myxomycete records for Turkey: One new Genus and three new species. Turkish Journal of Botany 32: 329-332, 2008.

H. Baba, Ç. Arslan, ‘‘Myxomycetes of North Amanos Mountains (Hatay/Turkey),’’ *Biological Diversity and Conservation*, 10(3) 88-95, 2017b.

H. Baba, M. Gelen, M. Zümre, ‘‘Türkiye den ilk defa Fimikol Miksomiset kaydı,’’ *The journal of fungus*, 5(1): 1-6, 2014.

H. Baba, M. Zumre, M. Gelen, ‘‘An Investigation on North Adana (Turkey) Myxomycetes,’’ *Chiang Mai Journal of Science*, 43(1): 54-67, 2016.

H. Baba, M. Zümre, M. Gelen, ‘‘Biodiversity of Kuseyr Plateau Myxomycetes (Hatay-Turkey),’’ *Journal of Selcuk University, Natural and Applied Science, Special Issue, ICOEST Conf. 2013 (Digital Proceeding of the International Conference on Environmental Science and Technology – 2013, Cappadocia, Turkey, 18–21 June 2013) (Part 1)*, 669–683, 2013.

H. Baba, Y. Doğan, ‘‘Investigation of Myxomycetes (Myxomycota) in South Amanos Mountains (Hatay-Turkey),’’ *Celal Bayar University Journal of Science*, 14(3): 277-284, 2018.

H. Baba, M. Gelen, M. Sevindik, “Taxonomic investigation of myxomycetes in Altınözü, Turkey,’’ Mycopath, 16(1): 23-31, 2018.

H.W. Keller, K. Braun, ‘‘Myxomycetes of Ohio: Their Systematics, Biology and Use in Teaching,’’ Ohio Biological Survey, Columbus, 1999.

I. Kalyanasundaram, ‘‘Myxomycetes in the tropics: distribution and ecology,’’ p. 227–237 in K. K. Janardhanan, C. Rajendran, K. Natarajan, and D. L. Hawksworth, editors. Tropical mycology. Science Publishers, Inc., Enfield, New Hampshire, 1997.

M. Blackwell, R.L. Gilbertson, ‘‘Sonoran desert myxomycetes,’’ *Mycotaxon*, 11: 139-149, 1980.

M. Schnittler, S.L. Stephenson, ‘‘Myxomycete biodiversity in four different forest types in Costa Rica,’’ *Mycologia*, 92, 626-637, 2000.

M.F. Madelin, ‘‘Methods for studying the ecology and population dynamics of soil myxomycetes,’’ *Methods in Microbiology,* 22: 405-416, 1996.

M.L. Farr, ‘‘Flora Neotropica Monograph No. 16 Myxomycetes,’’ New York Botanical Garden, New York, 1976.

S. Stephenson, ‘‘Distribution and ecology of myxomycetes in temperate forests. II. Patterns of occurrence on bark surface of living trees, leaf litter, and dung,’’ *Mycologia*, 81: 608-621, 1989.

S.L. Stephenson, A.M. Fiore-Donno, M. Schnittler, ‘‘Myxomycetes in soil,’’ *Soil Biology and Biochemistry*, 43: 2237–2242, 2011.

S.L. Stephenson, H. Stempen, H., ‘‘Myxomycetes, a Handbook of Slime Molds’’ Timber Press, Portland, Oregon, 1994.

U.H. Eliasson, ‘‘Coprophilous myxomycetes: recent advances and future research directions,’’ *Fungal Divers*., 59: 85–90, 2013.

U.H. Eliasson, N. Lundqvist, ‘‘Fimicolous myxomycetes,’’ *Bot. Notiser*, 132: 551-568, 1979.

PHARMACOLOGICAL ACTIVITIES OF PYRIMIDINE DERIVATIVE DRUGS

Nurcan BERBER[1]

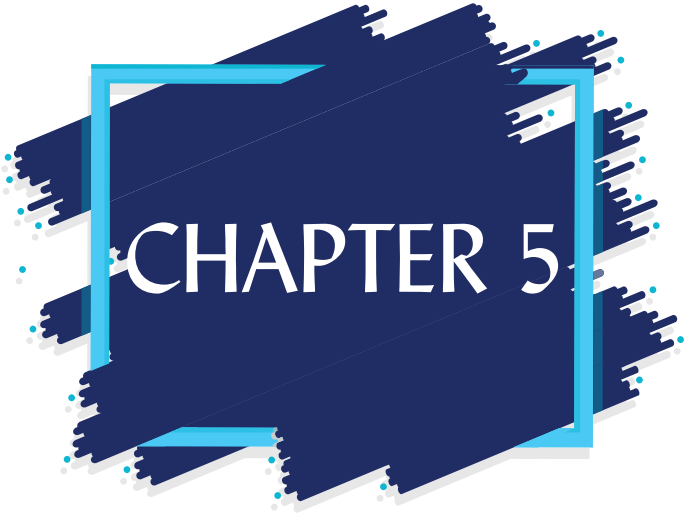

1 Department of Food Technology, Ezine Vocational School, Çanakkale 18 Mart University, Çanakakale, 17600, TURKEY

PHARMACOLOGICAL ACTIVITIES OF PYRIMIDINE DERIVATIVE DRUGS

Nurcan BERBER[1]

INTRODUCTION

Heterocyclic compounds are a major class of organic chemical compounds. They are those having five- or six-membered rings and containing heteroatoms of nitrogen (N), oxygen (O), or sulfur (S). They offer a high degree of medicinal importance and one of the most important their are pyrimidines that with six-membered heterocyclic ring [1,2,3]. The pyrimidines moisture compounds are an important component in natural products because of their pronounced biological activity. For example, It contains the uridine, deoxythymidine, and cytidine pyrimidine ring which form the main structure of the nucleoside bases necessary for the synthesis of DNA and RNA (Figure 1) [4, 5]. Uridine has been successfully used by the anti-cancer agent 5-fluorouracil as a protective or salvage agent against host toxicity [6,7].

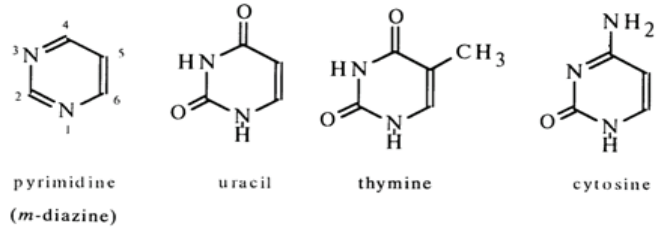

Figure 1. *Structure of Pyrimidine-Based nuckleosides.*

In the last two decades uracil and oxopyrimidine derivatives have been investigated extensively in relation to their antiviral and antitumoral properties [8] So that, it is a

1 Department of Food Technology, Ezine Vocational School, Çanakkale 18 Mart University, Çanakakale, 17600, TURKEY

usual building block in the synthesis of pharmacologically active compounds [9-13].

Certain pyrimidines and annulated pyrimidines derivatives continue to attract broad interest because of their structural diversity and association with a wide spectrum of biological activity [14] such as anticancer [15,16], antiviral [17], antitumor [18], anti-inflammatory [19], anti-depressive [20] and antimicrobial activities [21]. Some biologically active important pyrimidine derivative compounds are shown in (Figure 2). From these compounds flucytosine **(1)** is a fluorinated pyrimidine and is an orally active antifungal agent [22, 23], amicetin **(2)** is activity against bacteria [21]. The other pyrimidine derivatives **(3), (4)** and **(5)** have antibacterial and antifungal properties. Some biologically active pyrimidine derivatives were given Figure 2 [24-27].

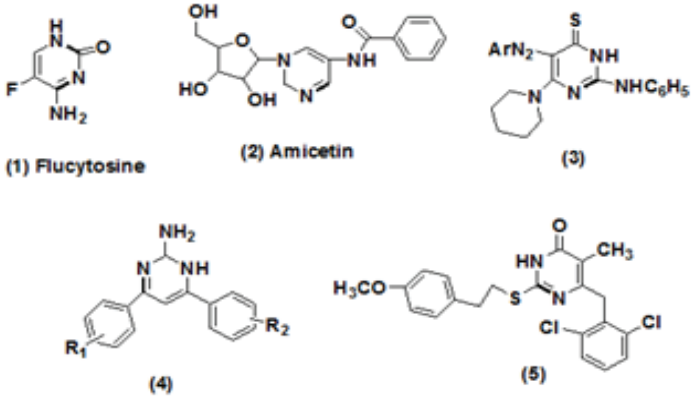

Figure 2. *Some biologically active pyrimidine derivatives.*

Recently, the synthesis of pyrimidine derivatives could be easily made by employing the multicomponent reaction (MCR) method [28,29] This method has become an important area of research in organic, combinatorial, and medicinal chemistry, because it can dramatically reduce

the generation of chemical waste and the costs associated with reactions [30,31]. As known reactions, such as Ugi reaction [32], Mannic reaction [33] and Biginelli reaction [34,35] etc. can be given as examples for Multi-component reactions. In 2011, Sagi and coworkers synthesised biological evaluation of novel pyrimidine derivatives as sub-micromolar affinity ligands of GalR2 (Figure 3) [36]. Also, Li et al. synthesised 2-alkylthio-4-amino-5-cyano-6-aryl(alkyl)pyrimidines 2012 [37]. Also, Li et al. synthesised 2-alkylthio-4-amino-5-cyano-6-aryl(alkyl) pyrimidines 2012 [37].

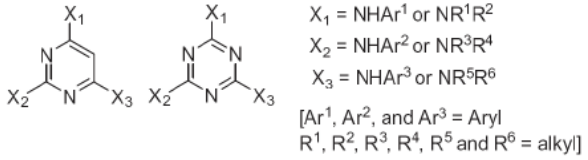

Figure 3. *Structures of 4 (CYM2024) and general structures of 2,4,6-triamino pyrimidines and triazines.*

Nia and colleagues coupled Synthesis of pyrido[2,3-d]pyrimidine-4,7(3H,8H)-diones (Figure 4) [38]. Anwar et al. exploited new pyrimidine derivatives with antitumor and antioxidant (Figure 4) [39]. Mikulewicz et al. revealed antibacterial properties of new pyrimidine derivatives [40].

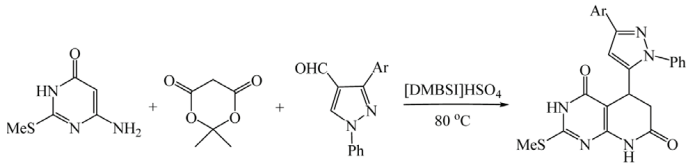

Synthesis of pyrido[2,3-d]pyrimidine-4,7(3H,8H)-diones

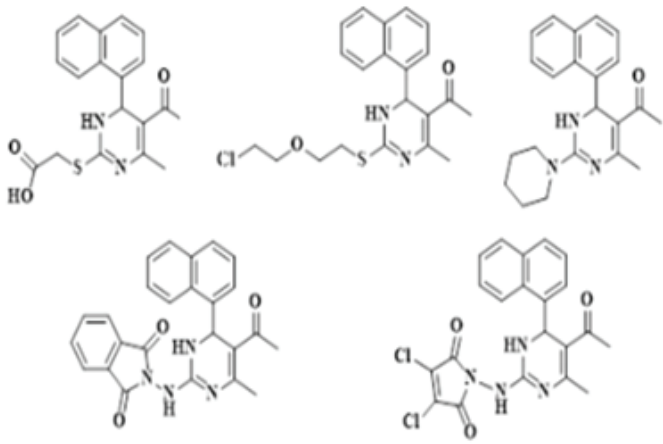

Figure 4. *new pyrimidine derivatives whith antitumor and antioxidant*

In another novel route, Kalla et al. described the synthesis of xanthene and pyrimidine-fused heterocyclic derivatives showing antioxidant properties (Figure 5) and product yield was quite high [41].

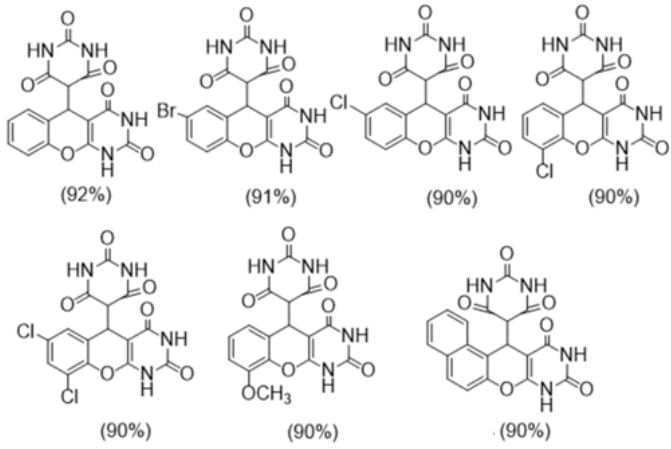

Figure 5. *Catalyst-free synthesis of pyrimidine-fused heterocyclic derivatives showing antioxidant properties.*

Pharmacological Activities Pyrimidine Drugs

The pyrimidine derivatives have supposed as essential part in nucleic bases, vitamins, enzymes, hormones and moreover the broad spectrum of pharmaceutical properties. They acquire pharmacological properties according to the functional groups that binding to the pyrimidine ring or the binding positions of these groups. Panneerselvam et al. had reported that 2nd position of pyrimidine ring six or five membered saturated heterocyclic ring substitution leads to anthelmintic, antiparkinson etc., or 2nd and 4th position keto/amino group substitution leads to anticancer, antiviral, antibacterial, antifungal etc. [42]. Some important pyrimidine drugs informations; drug's name, chemical structure and biological activities were given in Figure 6.

Antibacterial

Trimethoprim

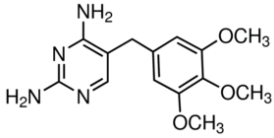

Tetroxoprim

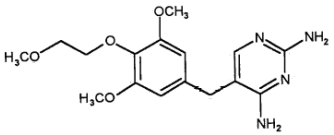

Piromidic Acid

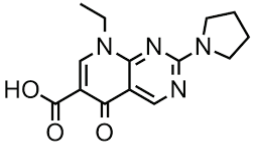

Antifungal

Flucytosine

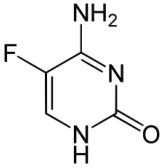

Antiviral

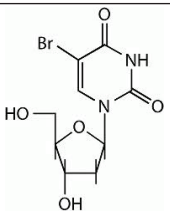

Broxuridine

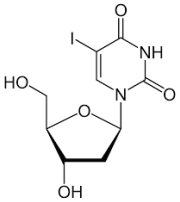

Idoxuridine

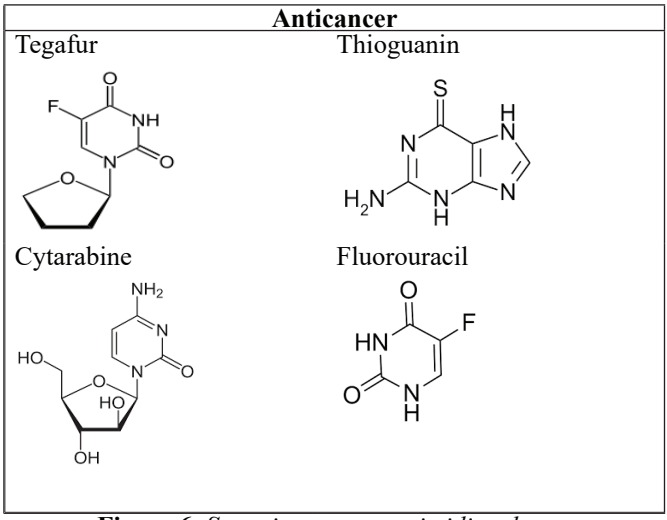

Figure 6. *Some important pyrimidine drugs.*

CONCLUSION

This study reveals that successful synthesis of new derivatives of pyrimidine with different chemicals and many of them were shown pharmacological activities such as antibacterial, antifungal, anticancer activities and so many [43-45]. I have herein reviewed recent advances in the chemistry and biology of pyrimidine in order to provide valuable information on how could be used to develop new drugs.

REFERANCE

1. Keche, A.P, et al. "Novel pyrimidine derivatives with aryl urea, thiourea and sulfonamide moieties: synthesis, anti-inflammatory and antimicrobial evaluation." Bioorganic & Medicinal Chemistry, 2012; 22:3445–3448.

2. Zijian, L., et al. "Design, synthesis and biological evaluation of novel thieno [3,2-d] pyrimidine derivatives containing diaryl urea moiety as potent antitumor agents." European Journal of Medicinal Chemistry, 2014; 85:215–227.

3. Anupama, B., et al. "Synthesis and antimicrobial activity of some new 2,4,6-trisubstituted pyrimidines. " International Journal of Research in Pharmacy and Chemistry, 2012; 2(2):231–236

4. Salway, J.G., "Medical biochemistry at a glance." Wiley-blackwell, 2012; 62:124-130.

5. Agarwal, N., et al. "Chloropyrimidines as a newclass of antimicrobial agents." Bioorganic & Medicinal Chemistry, 2002;10: 869-874.

6. Seiter, K., et al. "Uridine allows dose escalation of 5-fluorouracil when given with N-phosphoancetyl-L-aspartate, methotrexate, and leucovorin." Cancer, 1993; 71: 1875–1881.

7. Groeningen, C.J., Peters, G.J., Pinedo, H.M., "Modulation of fluorouracil toxicity with uridine." Seminars in Oncology, 1992; 19: 148-54.

8. Mohamed, K.S., Abdulaziz, N.M., Fadda, A.A., "Synthesis of some new pyridine and pyrimidine derivatives containing benzothiazole moiety." Journal of Heterocyclic Chemistry, 2013; 50: 645-649.

9. Sharma, V., Chitranshi, N., Agarwal, A.K., "Significance and biological importance of pyrimidine in the microbial world." Hindawi, 2014;2014:202784. (doi:10.1155/2014/202784)

10. El-Gazzar, A.R., Hussein H.A., Hafez, H.N. "Synthesis and biological evaluation of thieno[2,3-d]pyrimidine

derivatives for anti-inflammatory, analgesic and ulcerogenic activity." Acta Pharmaceutica, 2007;57:395–411.

11. Singh, K., Swanson, B., Moreland, S., "Dihydropyrimidine angiotensin II receptor antagonists." Journal of Medicinal Chemistry, 1992;35:4751-4763.

12. Singh, K., Swanson, B., Moreland, S., "Dihydropyrimidine calcium channel blockers as orally effective antihypertensive agents." Journal of Medicinal Chemistry, 1991;34:806-811.

13. Lanjewar, K., et al.,"Synthesis and antimicrobial activity of some dihydropyrimidines." Indian Journal of Chemistry, 2009;48:1732-1737.

14. Hanusek, J., et al. "Synthesis of substituted 2-benzoylaminothiobenzamides and their ring closure to substituted 2-phenylquinazoline-4-thiones." Molecules 2001;6:323-337.

15. Kaldrikyan, M.A., et al. "Synthesis and antitumor activity of some disubstituted 5-(3-methyl-4-alkoxybenzyl)-pyrimidines." Pharmaceutical Chemistry Journal, 2000;34:521−524.

16. Lefebvre, C.A., Forcellini, E., Boutin, S., "Synthesis of novel substituted pyrimidine derivatives bearing a sulfamide group and their in vitro cancer growth inhibition activity." Bioorganic & Medicinal Chemistry, 2017;27:299-302.

17. Nasr, M.N., Gineinah, M.M., "Pyrido[2,3-d]pyrimidines and pyrimido[5',4':5,6]-pyrido[2,3-d] pyrimidines as new antiviral agents: synthesis and biological activity." Acta Pharmaceutica, 2002;335:289–295. (doi:10.1002/1521-4184(200208)335:6289)

18. Baraldi, P.G., et al. "Antimicrobial and antitumor activity of N-heteroimine-1,2,3-diathiazoles and their transformation in triazolo-, imidazo- and pyrazolopyrimidines." Bioorganic & Medicinal Chemistry, 2002;10:449–456.

19. Sondhi, S.M., Johar, M., Rajvanshi, S., "Anticancer, anti-inflammatory and analgesic activity evaluation of

heterocyclic compounds synthesized by the reaction of 4-isothiocyanato-4-methylpentan-2-one with substituted o-phenylenediamines, o-diaminopyridine and (un) substituted o-diamino-pyrimidines." Australian Journal of Chemistry, 2001;54:69–74.

20. Lewis, R.W., et al. "Dihydropyrimidinone positive modulation of δ-subunit-containing γ-aminobutyric acid type a receptors, including an epilepsy-linked mutant variant." Biochem, 2010;49:4841–4851.

21. Chowdhury, A.Z.M.S., Matin M.M., Anwar, M.N., "Synthesis and antimicrobial activities of fused pyrimidines: benzothieno[2,3-d]imidazol[1,2-c]pyrimidine." Chittagong Univ. Stud. Part II, 1997;21:79–83.

22. Smith, J., Andes, D., "Therapeutic drug monitoring of antifungals: pharmacokinetic and pharmacodynamic considerations." Therapeutic Drug Monitoring, 2008;30:167-172.

23. Chadwick, B., Addy, M., Walker, D.M., "Hexetidine mouthrinse in the management of minor aphthous ulceration and as an adjunct to oral hygiene," British Dental Journal, 1991;171:83–87.

24. Reddick, J.J., et al. "The mechanism of action of bacimethrin, a naturally occurring thiamin antimetabolite," Bioorganic & Medicinal Chemistry, 2001;11:2245–2248.

25. Aly, A.A., Nassar, S.A., "N-[4-(dicyanomethylazo)phenyl]-2-saccharin-2-ylacetamide in the synthesis of pyridazine and pyrimidine derivatives," Heteroatom Chemistry, 2004;15:2–8.

26. Pasha, T.Y., Udupi, R.H., Bhat, A.R., "Synthesis and antimicrobial screening of some pyrimidine derivatives," Indian Journal of Heterocyclic Chemistry, 2005;15:149–152.

27. Manetti, F., et al. "Parallel solutionphase and microwave-assisted synthesis of new S-DABO derivatives endowed with subnanomolar anti-HIV-1 activity." Journal of Medicinal Chemistry, 2005;48:8000–8008.

28. Kidwai, M., Singhal, K., Kukreja, S. "One-pot green synthesis for pyrimido [4, 5-d] pyrimidine derivatives. " Zeitschrift für Naturforschung B, 2007;62(5):732-736.

29. Tan, S.H., Chuah, T.S., Chia, P.W. "An improved protocol on the synthesis of thiazolo [3, 2-a] pyrimidine using ultrasonic probe irradiation." Journal of the Korean Chemical Society, 2016;60(4):245-250.

30. Robert W.A., et al. "Multiple-component condensation strategies for combinatorial library synthesis." Accounts of Chemical Research, 1996;29:123-131.

31. El-Asri, Z., et al. "Multicomponent reactions in ionic liquids: convenient and ecocompatible access to the 2,6-DABCO core." Green Chemistry, The Royal Society of Chemistry, 2011;13:2549-2552.

32. Sunderhaus, J.D., Martin, F. S., "Applications of multicomponent reactions to the synthesis of diverse heterocyclic scaffolds." Chemistry, 2009;15(6):1300–1308. (doi:10.1002/chem.200802140)

33. Subramaniapillai, S.G., "Mannich reaction: a versatile and convenient approach to bioactive skeletons." Journal of Chemical Sciences, 2013;125(3):467–482.

34. Suresh and Sandhu J.S., " Past, present and future of the Biginelli reaction: a critical Perspective." Arkıvoc, 2012;(i):66-133.

35. Gawarea, M.R., et al., "A simple and efficient one pot synthesis of. 2,4 dioxopyrimidine carbonitrile and 4-oxo-2-thioxopyrimidine carbonitrile derivatives using ammonium chloride under solvent free conditions. " International Journal of Cardiology, 2017;56;997-999.

36. Sagi, V.N., et al. "Synthesis and biological evaluation of novel pyrimidine derivatives as sub-micromolar affinity ligands of GalR2." Bioorganic & Medicinal Chemistry letters, 2011;21(23):7210-7215.

37. Li, Q.Y., et al. "An efficient three-component, one-pot synthesis of 2-alkylthio-4-amino-5-cyano-6-aryl (alkyl) pyrimidines in water." Molecular Diversity, 2012:16(3):431-439.

38. Nia, R.H., et al. (2014). “A rapid one-pot synthesis of pyrido [2, 3-d] pyrimidine derivatives using brřnsted-acidic.” Acta Chimica Slovenica, 2014:60(4):889-895.

39. Anwar, M.M., et al. “New pyrimidine derivatives: synthesis, antitumor and Antioxidant evaluation.” International Journal of Pharmacy & Technology, 2015;7(1): 8061-8085.

40. Cieplik, J., et al. “Synthesis and antibacterial properties of pyrimidine derivatives.” Acta Poloniae Pharmaceutica, 2011;68(1):57-65.

41. Naidu Kalla, R.M.,et al. “Catalyst-free synthesis of xanthene and pyrimidine-fused heterocyclic derivatives at water-ethanol medium and their antioxidant properties.” Chemistry Select, 2019;4(2):644-649.

42. Selvam, T.P., et al. “A mini review of pyrimidine and fused pyrimidine marketed drugs.” Research in Pharmacy, 2012; 2(4):01-09.

43. Abdelrahman, M.A., et al. Design, synthesis and 2D QSAR study of novel pyridine and quinolone hydrazone derivatives as potential antimicrobial and antitubercular agents. European Journal of Medicinal Chemistry, 2017;138:698-714.

44. Kumar, S., et al. Bis-pyrimidine acetamides: design, synthesis and biological evaluation. Chemistry Central Journal, 2017;11(1):80.

45. Mahfoudh, M., et al. Recent approaches to the synthesis of pyrimidine derivatives. European Journal of Organic Chemistry, 2017;2017(20):2856-2865.

GECE AKADEMİ

www.gecekitapligi.com

/gecekitapligi
/gecekitapligi
/gecekitap

9 786058 022942